aerospace

Article

# Numerical Simulation of Chemical Propulsion Systems: Survey and Fundamental Mathematical Modeling Approach

**Jihyoung Cha**

Department of Computer Science, Electrical and Space Engineering, Luleå University of Technology, Bengt Hultqvistsväg 1, 98192 Kiruna, Sweden; jihyoung.cha@ltu.se

**Abstract:** This study deals with the mathematical modeling and numerical simulation of chemical propulsion systems (CPSs). For this, we investigate and summarize a comprehensive collection of the simulation modeling developments of CPSs in academic works, applications, and industrial fields. Then, we organize and analyze the simulation modeling approaches in several ways. After that, we organize differential-algebraic Equations (DAEs) for fundamental mathematical modeling consisting of the governing Equations (ordinary differential equations, ODEs) for the components and other equations derived from several physical rules or characteristics (algebraic equations or phenomenological equations, AEs) and then synthesize and summarize the fundamental structures of analytic mathematical modeling by types (liquid-propellant rocket engines, solid-propellant rocket motors, and hybrid-propellant rocket motors) of CPSs.

**Keywords:** chemical propulsion system; solid-propellant rocket motor; hybrid-propellant rocket motor; liquid-propellant rocket engine; thermodynamic systems; mathematical modeling; review

check for updates

**Citation:** Cha, J. Numerical Simulation of Chemical Propulsion Systems: Survey and Fundamental Mathematical Modeling Approach. *Aerospace* **2023**, *10*, 839. https://doi.org/10.3390/aerospace10100839

Academic Editor: Jae Hyun Park

Received: 28 August 2023
Revised: 22 September 2023
Accepted: 23 September 2023
Published: 26 September 2023



## 1. Introduction

Due to recent developments in space system technologies and expanded approaches to space made possible by small satellite (SmallSat) technologies, new launch service providers, and international collaborations, a new space age, sometimes called Space 2.0, has emerged [1–3]. As a result, new technology encourages change in how the space industry operates, and the market for commercial launch services has expanded to put satellites into orbit. Therefore, one of the primary concerns is the low-cost commercialization and management of space launch vehicles (SLVs) to strengthen the competitiveness of the new space age [4–10]. However, the development cost for a new propulsion system is expensive, and there is a risk of accidents in development and tests. Furthermore, as a reusable launch vehicle (RLV) has become necessary, the maintenance of the RLV has also been a technical issue for a competitive price [11].

In the new space age, as the space market has moved from government-centered to commercial-centered, new requirements for new SLVs have emerged: long-life design methodology, a technique to evaluate the remaining lifetime, non-destructive inspection technology, and fault detection and diagnosis [12]. In developing a new SLV, numerous tests of the new propulsion system under various conditions are required to construct a dataset to satisfy these requirements. However, several tests cost a large expenditure of money, and a severe accident may occur in tests. Furthermore, as the experiments are repeated, inherent unknown damages can also accumulate from numerous tests. Furthermore, in the RLV case, as with aircraft engines, the RLV propulsion system must be ready for the next flight quickly because its inspection process before launch generally requires some disassembly, considering the tradeoff between reliability and maintenance costs. As a result, the fault simulation using the system-level model-based simulation is essential to reduce the number of tests by substituting the actual experiment and to generate a database for the failure mode and effect analysis (FMEA) for constructing a reliable health monitoring system [12–18]. Therefore, the above advantages of developing a reliable simulation program can be summarized:

- Shortening the development period and reducing development cost.
- Protect potential problems and predict propulsion performance in various conditions.
- Generate a database for the possible failure modes from FMEA and develop a reliable health monitoring system.
- Reduce maintenance cost for RLVs.

Due to the above advantages, interest in simulation programs has increased significantly recently. However, developing a simulation program is difficult because of the complexity of a chemical propulsion system (CPS), especially for a liquid-propellant rocket engine (LPRE). Additionally, because system-level simulation models use reduced-order models of each component and require specifying numerous model parameters, reliable experimental data obtained from physical model testing are essential to ensure the reliability of the simulation model. However, in the case of a CPS, it is difficult to obtain data for each component due to security issues. Therefore, developing a reliable mathematical simulation program requires collaboration with various research institutes or teams to secure experimental data of an actual system, and it is challenging to conduct related research because it takes a lot of time.

Many studies have been conducted with system-level mathematical modeling to predict the performance of rocket propulsion systems. In the beginning, the primary use of simulation modeling in LPREs is to predict the transient state and design point in the preliminary and critical design process, while solid-propellant rocket motors (SPRMs) and hybrid-propellant rocket motors (HPRMs) are generally for the design control system. At that time, the RL10A-3-3A engine, employing an expander cycle, was often used to verify system-level simulation modeling [12]. However, these days, as the computation and rocket technical skills have been improved, the main objective of simulation modeling has been expanded to make a dataset for upgrading and preparing the next-generation engine or developing health monitoring systems. The system-level simulation modeling has also been developed for various types of CPSs, such as LPREs, SPRMs, and HPRMs, by applying diverse cycle types in LPREs, such as expander cycle, staged-combustion cycle, gas-generator cycle (also called open-cycle), and recently, electric-pump-fed cycle. However, there are no comprehensive studies showing that a CPS dynamics can be derived from the same governing equations. Therefore, this study aims to investigate and analyze system-level simulation modeling trends and synthesize and organize approaches to a CPS.

The following section briefly overviews of CPSs. Section 3 surveys and reviews the dynamic simulation program of CPSs and analyzes the trends by perspectives. Then, Section 4 summarizes and organizes the dynamic equations depending on the types of a CPS. Finally, Section 5 concludes this study.

## 2. Overview of Chemical Propulsion Systems

The rocket propulsion system is a system that generates thrust by expelling exhaust fluid accelerated at high speed through a nozzle using stored rocket propellants as the reaction mass based on Newton's third law of motion [19–21]. Rocket propulsion systems can be classified into chemical (liquid, solid, and hybrid) and non-chemical (electrical, thermal, solar, and nuclear) types, as shown in Figure 1. For high propulsion for launch, the most useful energy source for rocket propulsion is CPSs because the systems have several advantages for a multistage system: the propellants can be safely stored, the thrust–weight ratio is generally higher than in non-chemical propulsion systems, and the combustion process results in a great deal of heat being released, as shown in Table 1 [19–21].

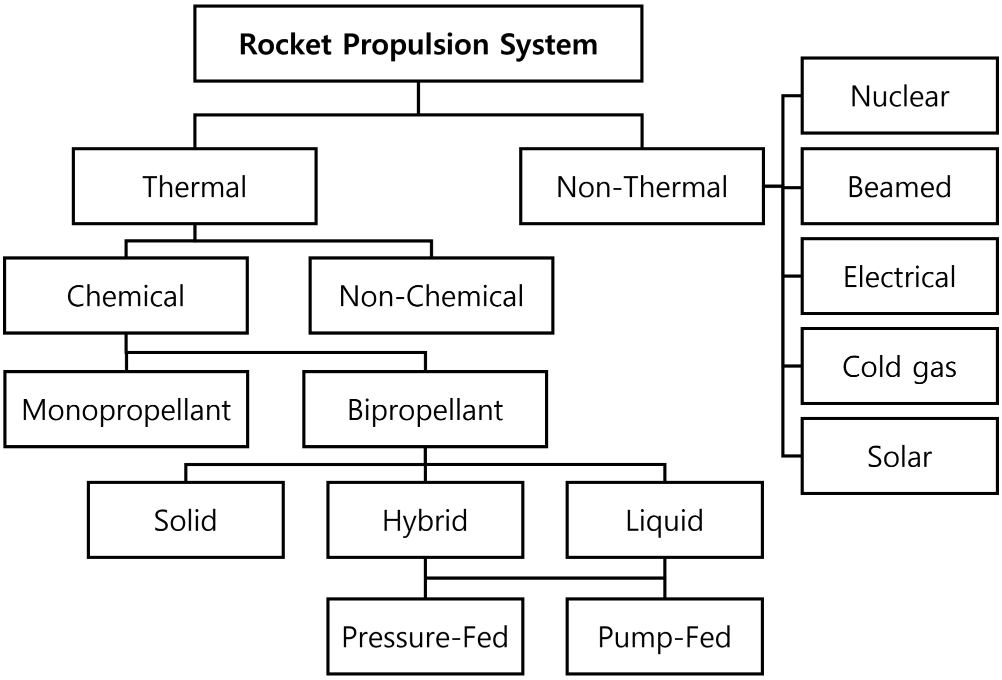


**Figure 1.** Classification of rocket propulsion systems (Reprinted with permission: El-Sayed, A. F. Fundamentals of Aircraft and Rocket Propulsion, Copyright © 2018 by the Springer with permission [22].)

**Table 1.** Comparison of rocket propulsion systems [20,22].

| Types | Specific Impulse | Thrust/Weight Ratio | Thrust Duration |
|---|---|---|---|
| Chemical Rocket | 170–465 | 1–10 | Minutes |
| Electrothermal | 300–1500 | $<10^{-3}$ | Months (steady) Years (intermittent) |
| Electromagnetic | 1000–10,000 | $<10^{-4}$ | Months (steady) Years (intermittent) |
| Electrostatic | 2000–100,000 | $<10^{-4}$–$10^{-6}$ | Months/years (steady) |
| Nuclear (thermal) | 750–1500 | 1–5 | Hours |

The CPSs can be categorized into SPRMs, HPRMs, and LPREs, depending on the state of the oxidizer and fuel, as shown in Figure 2 [19,21].

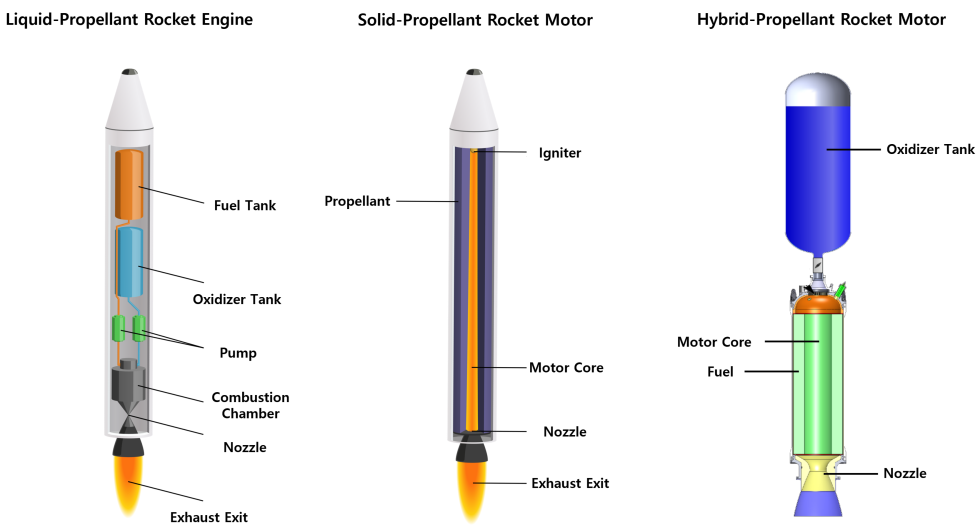


**Figure 2.** Classification of rocket propulsion systems.

Liquid propellant rocket engines (LPREs) use liquid propellant supplied under pressure or pumped from a tank into the thrust chamber. LPREs can consist of a single chemical (a monopropellant) or a mix of two chemicals (a bipropellant). A monopropellant is a single liquid containing both an oxidizer and a fuel species, whereas a bipropellant consists of liquid fuel (e.g., kerosene, liquid hydrogen) and liquid oxidizer (e.g., liquid oxygen) [19,21,23]. There are other ways to categorize them, such as based on propellants (cryogenic, semi-cryogenic, and non-cryogenic) and cycles (pressure-fed, gas-generator, expander, staged-combustion, and recently electric pump-fed), as shown in Figure 3 [23]. One of the powerful advantages of an LPRE is that it can be throttled in real time, and the mixing ratio (ratio between oxidizer and fuel) can be controlled. It can also be shut down and restarted using the appropriate ignition system.

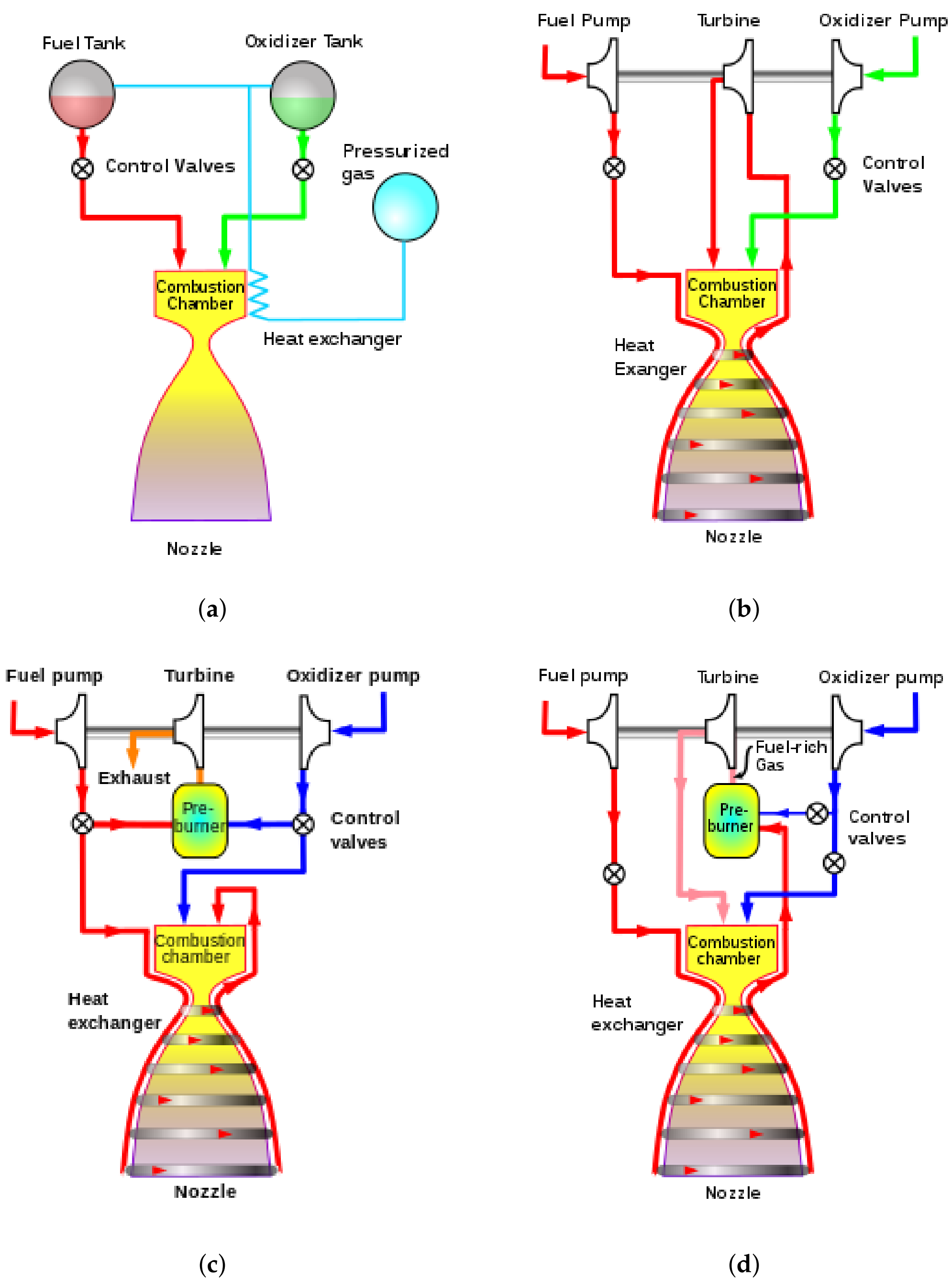


**Figure 3.** *Cont.*

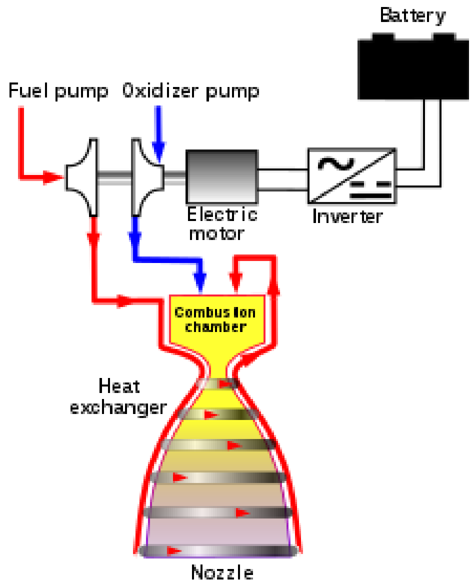


(e)

**Figure 3.** Liquid-propellant rocket engine cycles. (**a**) Pressure-fed cycle. (**b**) Expander cycle. (**c**) Gas-generator cycle. (**d**) Staged combustion cycle. (**e**) Electric-pump-fed cycle.

Solid propellant rocket motors (SPRMs) contain propellant to be burned within the combustion chamber. The solid propellant charge is called the grain and has all the chemical elements necessary for complete burning. Once ignited, it usually burns smoothly at a predetermined rate over all exposed inner surfaces of the grain. As the propellant is burned and consumed, the internal cavity grows, and the generated hot gas flows through a supersonic nozzle to generate thrust until all the propellant is consumed [19,21,24].

Hybrid propellant rocket motors (HPRMs) use both liquid and solid propellants by mixing a liquid oxidizer and a solid fuel [19,25]. This concept allows throttling, shutdown, and restart until all the solid propellant is consumed, but this is not possible with SPRMs. It is also possible to use a liquid fuel and a solid oxidizer, called a reverse HPRM [21].

## 3. Simulation Modeling Trend of Chemical Propulsion Systems

### *3.1. Literature Review*

Various studies have been conducted to develop mathematical simulation models of a CPS, and simulations have been applied to collect data under various conditions for low development costs and multiple purposes. In addition, the simulation approach can prevent an unknown inherent defect that accumulates over numerous repeated actual tests and can cause a severe fault in-flight.

In previous research and space-advanced countries, mathematical simulation models have been developed mainly focusing on an LPRE, because an LPRE is much more complex than others, and most developed simulation models have focused on large thrust with controllability. In the case of SPRMs or HPRMs, since the system structure of SPRMs or HPRMs is relatively safe and simple compared to LPREs, a simulation model has been developed to use experimental approaches or realistic systems simultaneously or to design control systems. Then, because more than 30% of the engine failures occurred during the start-up process, such as propellant feed system failure, turbopump failure, and defective welding of the seam holding a cover, researchers have begun to recognize the importance of accurately modeling under a transient state, especially the start-up process [26,27]. Therefore, we investigate simulation models for LPREs, SPRMs, HPRMs, and the transient state in this subsection.

#### 3.1.1. Liquid-Propellant Rocket Engines

The space-advanced countries developed simulation programs mostly for LPREs by developing their own SLVs. Typical examples are rocket engine transient simulation (ROCETS) developed by Pratt & Whitney in the U.S., consisting of thirteen component modules, and the rocket engine dynamic simulator (REDS) by Japan Aerospace eXploration Agency (JAXA), which is an upgrade version of ROCETS using partial differential Equation (PDE) to obtain nonlinear mass flow rate and heat transfer characteristics in the pipeline [28,29]. EcosimPro is also one of the representative programs used for a commercial program called European Space Propulsion System Simulation (ESPSS), employing a set of libraries containing various types of components that can be interconnected to model complex dynamic systems in Europe [30,31]. Using the libraries of the ESPSS, the SPRMs and HPRMs can also be developed [32].

Additionally, many research groups in institutes and universities have developed their own program or improved each component model and added it to the libraries through research focusing on each component through numerical simulation and experiment. In the U.S., Rocketdyne developed a thermodynamic model for the space shuttle main engine (SSME) [33]. In Ref. [33], although the equations were purely descriptive, there was no analysis and understanding of the physical phenomena of the engine, such as several constant coefficients meaning in dynamic equations and not clarifying the origin of the equations. For this, the Massachusetts Institute of Technology (MIT) analyzed and derived the dynamic equations and applied them to develop a fault detection and diagnosis (FDD) algorithm [34–36]. However, since the models focused on only a steady state or quasi-steady state, the Aerospace Corporation developed an accurate transient state simulation model considering the water hammer phenomenon [37]. In Europe, in addition to ESPSS, research was also conducted to develop simulation models. The German Aerospace Center (DLR) researched simulation modeling to simulate the start-up of an LPRE considering various fluid flow phenomena (two-phase flow) and the numerical resolution of these phenomena [38,39]. Additionally, the France Space Agency (CNES) developed a simple thermodynamical simulator of an open-cycle LPRE in MATLAB/SIMULINK to capture a transient behavior and verified with the Vulcane 1 engine to design a thrust control algorithm [40,41]. In Russia, the Moscow Aviation Institute (MAI) presented a simulation program based on ANASYN for commercial programs to analyze transient behavior [42]. The NPO Energomash, a major Russian rocket engine manufacturer, also developed a self-production program using a simple dynamic equation complemented with experimental-based empirical Equations [43]. China also has started to study developing a simulation model in various institutes. The National University of Defense Technology (NUDT) developed a simple mathematical model for an open-cycle LPRE to study FDD algorithms [44–46]. After that, the university developed a tool called the Modularization Modeling and Simulation Software for the Transients of Liquid Propellant Rocket Engines (LRETMMSS) to study rocket engine transient states based on the decomposition method [47]. Huazhong University of Science and Technology (HUST) developed an LPRE model library in Modelica language that contains component models, such as pipes, valves, tanks, turbo-pumps, combustion chambers, nozzles, injectors, gas generators, etc. [48]. Using the library, various LPRE models, including gas-pressurized and pumped systems, can be established in a transient state [48]. The Beijing University of Aeronautics and Astronautics (BUAA) also developed a simulation model for quantitative analysis of an open-cycle LPRE and SSME with a modular approach. In the component library (including the thrust chamber, gas generators, turbines, pumps, pipelines, and valves), the stationary macroscopic behavior (typically including the pressure, temperature, flow rate, and power) of each module is simulated by the basic zero-dimensional analytical model with some empirical correlations [49–53]. In Brazil, the Institute of Aeronautics and Space (IAE) developed and reported a steady-state modeling and simulation program for an open-cycle LPRE using C++ programming [54]. In the case of the fluidic resistance element, the pressure loss was modeled through an empirical equation as a constant multiple of the combustion chamber pressure, and the pump, turbine, and combustion chamber were modeled through the logarithmic equation. It was verified with Vulcain, HM7B, and SSME engines and showed a low error rate despite the simple modeling method with an average of 4%, 2%, and 6% performance errors per component unit [54]. In Korea, the Korea Aerospace Research Industry (KARI) developed a simulation model of open-cycle LPRE in steady-state using a linearization approach and transient state using in-house code [55–57] and of staged combustion cycle LPRE using energy balance equations to check operating points [58]. Korea Aerospace University (KAU) also developed a simulation program using two kinds of LPRE, a steady state of staged-combustion cycle and a transient state of open-cycle LPREs, and modulized each component of the program [59–62]. In addition, to analyze the start-up characteristics of a staged-combustion engine, a staged-combustion engine power pack has been developed at Chungnam National University (CNU) [63,64]. As small-size LPRE has become necessary recently [65], Inha University also developed a simulation program focusing on an electric-pump-fed cycle engine and verified it with a water flow test [66,67]. In addition to that, The Khajeh Nasir Toosi University of Technology (KNTU) in Iran also developed a simulation model of an open-cycle LPRE using Borland C to predict the effects of changes in the design of considered engine and apply it to other LPREs and a staged combustion cycle LPRE collaborated with BUAA in China [52,68,69].

#### 3.1.2. Solid-Propellant Rocket Motor

SPRMs have simple structures consisting of a case, nozzle, grain (solid propellant), and igniter and are suitable for long-term storage without propellant degradation compared to other types of propellant systems, so they have been used for various applications, such as sounding rockets, missiles, and orbital rockets [19,70]. In the past, since the mathematical model of SPRMs was simple and easy to develop, it was sufficient to construct a simulation model assuming a first- or second-order linear system [19,20,22,24]. However, over the past two or three decades, as the study on a variable-thrust solid-propellant rocket motor (VTSRM) using a pintle valve has been conducted, as shown in Figure 4 [71–76], it has become essential to develop a mathematical simulation model to solve some uncertainties in changing system parameters by the moving pintle and limited range of the pintle motion, as shown in Figure 5 [77,78]. Therefore, several institutes developed a mathematical simulation model considering the combustion chamber volume change as combusting progressed and verified by a cold gas test to design a pressure and thrust control system [77–84]. Additionally, using the characteristics, it can be extended to a multi-nozzle system for divert and attitude control as a reaction control system (RCS), so a simulation model was also developed considering each nozzle throat area, and various control systems were designed through the simulation approach [85–91].

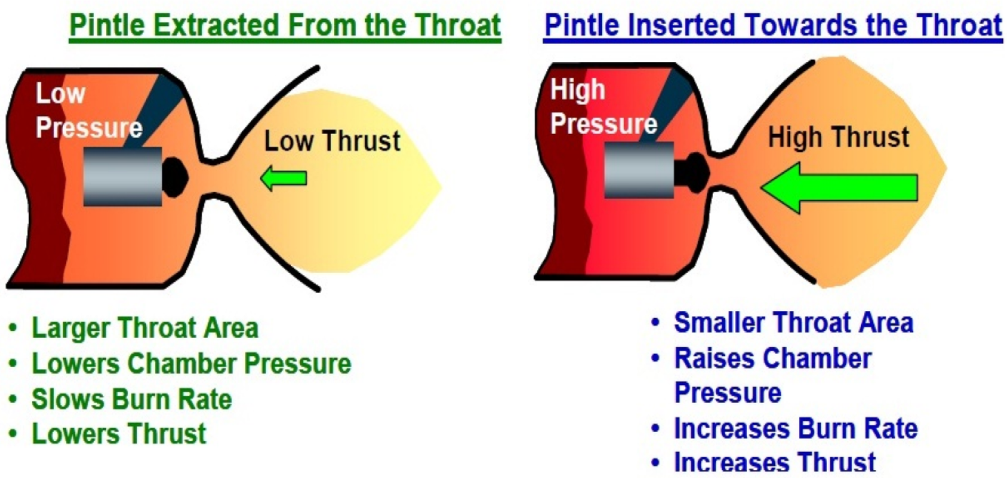


**Figure 4.** Pintle nozzle technology to control thrust by chamber pressure and throat area [73].

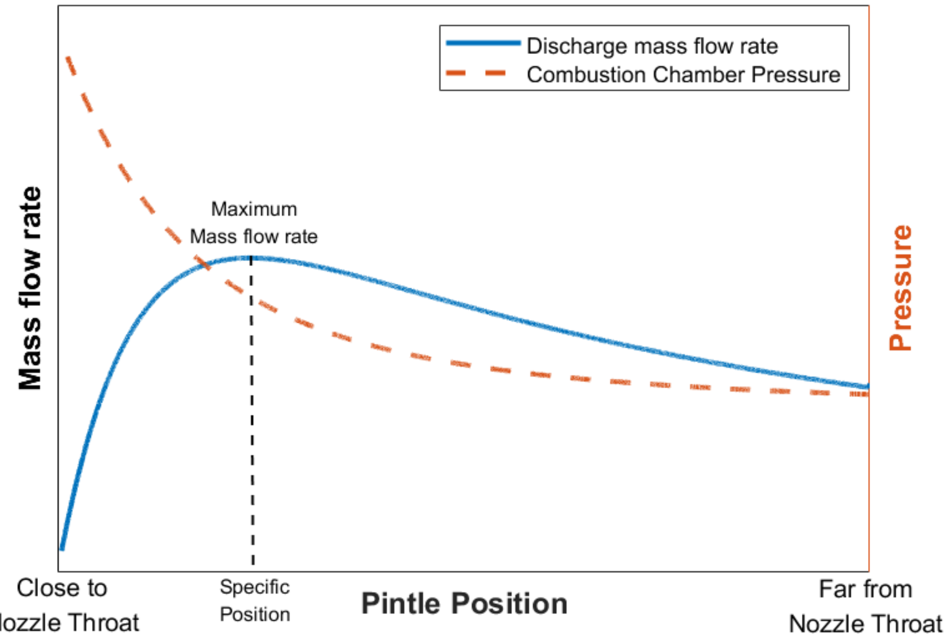


**Figure 5.** Discharge mass flow rate and pressure based on pintle position of a single-nozzle system [78].

Furthermore, recently, by applying a VTSRM, a simulation model of the ramjet or scramjet system, called dual-mode ramjet (DMRJ) or solid-fuel rocket scramjet (SFRSCRJ), has been developed and studied as a gas generator to generate and control the fuel-rich combustion gas, as in Figure 6 [92]. Since the fuel-rich combustion gas, generated from a VTSRM, is controlled by the pintle and makes variable thrust in the ram combustor, the characteristics of the system drive are one of several challenges in the DMRJ or SFRSCRJ, so a simulation model of SPRMs has been conducted to design an accurate control system for combustion gas flow rate [92–95].

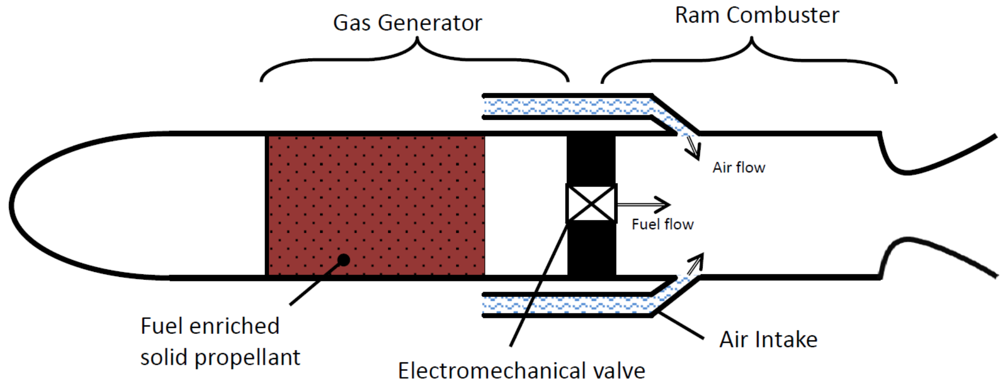


**Figure 6.** Schematic of a throttleable ducted rocket [92].

### 3.1.3. Hybrid-Propellant Rocket Motor

Since HPRMs are a system that combines the advantages of LPREs and SPRMs, HPRMs are capable of thrust control, safe, and simple, so research on HPRMs has been performed on a laboratory scale at universities or in countries starting space development. Because of the advantages of HPRMs, the performance can be predicted and verified through simultaneous simulation and experimental approaches [96–101]. Moreover, in recent years, since the private sector of the space industry has made significant advances as an independent supplier of launch rockets, which support national programs (construction of satellites, research equipment, etc.) and are mostly small launchers (also mini-launchers), HPRMs have become very promising for developing a small launch vehicle in this trend. For this reason, as the interest in HPRMs has increased significantly recently, the interest in developing an HPRM simulation model has also increased [9,102], and this interest has led to the development of simulation modeling of an HPRM to predict and evaluate its performance under various operating conditions [96–100,103,104]. In addition, vertical take-off and vertical landing (VTVL) has become one of the essential features of recent spacecrafts, so a simulation modeling approach has become important to design appropriate control algorithms because an HPRM has a simple structure and deep throttling capability [105]. Therefore, many researchers have developed a simulation model using a lumped model approach or appropriate linear identification and designed a control algorithm demonstrating the actual system [105–111]. Some European researchers also developed a simulation model of an HPRM using the ESPSS libraries and analyzed the performance of the HPRM [112,113].

#### 3.1.4. State of a Chemical Propulsion System

The operation of a CPS can be divided into a steady state, such as a design point or a specific operating point, and a transient state, such as start-up, shutdown, and thrust control. In general, the steady and transient states represent completely different hydrodynamic behaviors and are performed because the purpose of performance analysis is different. The purpose of steady-state performance analysis is to predict the performance of static characteristics and to analyze and determine the performance of each component and the overall system at the operating point of the CPS, mainly at the full thrust. Meanwhile, the purpose of transient performance analysis is to predict the performance of the dynamic characteristics of the fluid that occurs in the transient state of CPS according to changes in requirements, such as start-up or thrust changes. Generally, a transient state simulation is performed by changing from a specific operating point to a new one. Therefore, simulation modeling proceeds in the following order, as shown in Figure 7: steady-state performance analysis and transient-state performance analysis.

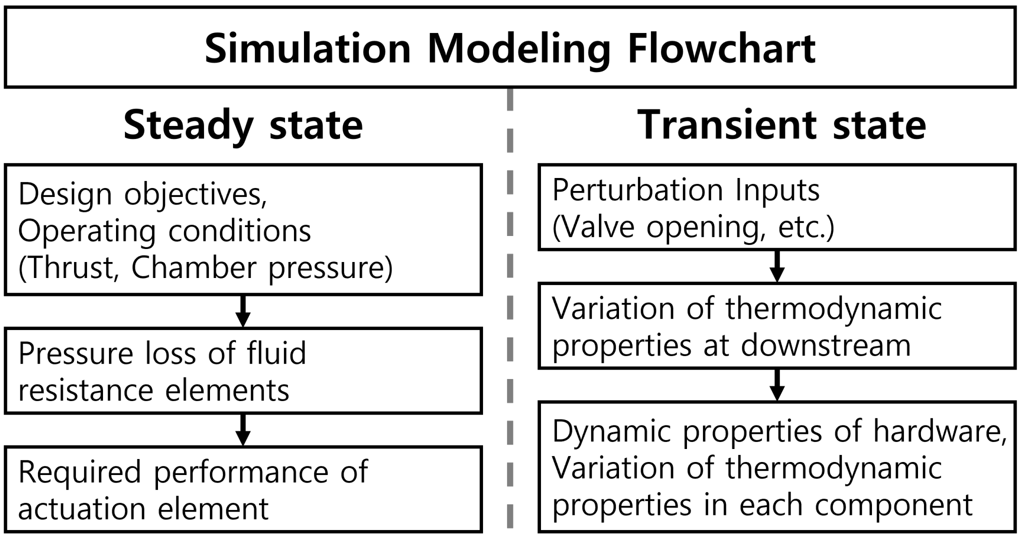


**Figure 7.** The flowchart of a steady/transient simulation modeling [17].

In the case of steady-state modeling, it is relatively simple to perform because there is no need to consider property changes in components over time. On the other hand, transient-state modeling is more complex than steady-state modeling because it requires information such as dynamic characteristics of components and phase changes of propellants. The property changes in each component interact with each other and ultimately cause combustion characteristics and thrust changes.

For the difficulties in transient-state modeling, various types of research were conducted focusing on the state changes in a transient state, especially the start-up process. In the nonlinear mass flow problem, Kalnin, V. M. and Sherstiannikov, V. A. arranged the scheme and the method of hydrodynamic modeling of the working process of an LPRE start-up process and presented an experimental investigation of the hydraulic system filling with the modeling liquid [26]. Lin. T. Y. and Baker, D. also performed analytical simulation modeling and experiments to analyze the nonlinear mass flow on the priming process of a propellant feed system with initial line pressures of zero condition and more with a simple tank-valve-pipeline system [114]. For the combustion instability problem, the combustion instabilities group at the DLR Lampoldshausen has worked to understand the thermoacoustic phenomena in LPREs for over one and a half decades [115]. As the European Arian 1 launcher suffered from combustion instabilities, a French-German research program was founded in 1999 and has worked towards understanding the combustion instability phenomena [116]. Schmidt et al. conducted an experimental and numerical simulation of the transient ignition phenomenology when igniting coaxial injected oxidizer and hydrogen by a laser. For this, they used high-speed photography for the temporal evolution of the flame and its anchoring at the injector and analyzed the movement of the flame and convection velocities [116]. In the initial condition and valve opening time problem, Bradley, M. performed the simulation with various initial conditions and opening time of each valve and analyzed the effects of the condition and performances with an SSME numerical simulation model [117]. Belyaev, E. N. et al. and Manfletti, C. independently studied the filling process in a pipeline, after a valve is opened, using simplified gas accumulator dynamics, where the primary underlying assumption is that there is no exchange between liquid and gas, as shown in Figure 8 [39,43].

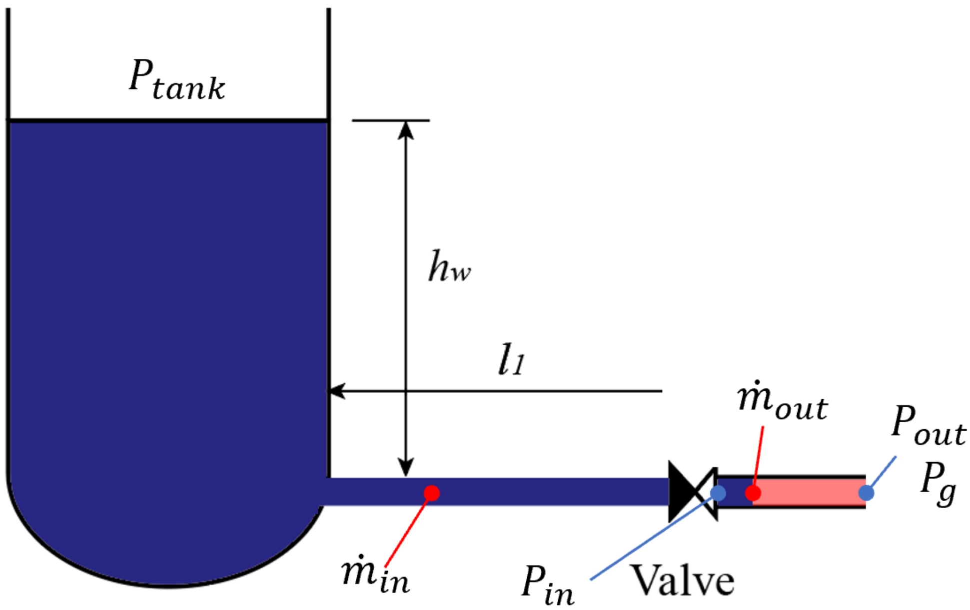


**Figure 8.** The filling process of pipelines

$$\bar{V}\frac{d}{dt}\dot{m}_{out} = \frac{A}{L}(P_{in} - P_{out} - K_m\dot{m}_{out}|\dot{m}_{out}|) \tag{1}$$

$$\bar{V} = \frac{V_{filled}}{V_{total}} \tag{2}$$

$$\frac{d}{dt}P_{out} = \begin{cases} \frac{d}{dt}P_g & \text{for} \quad 0 \leq \bar{V} < 1 \\ \frac{a^2}{V}(\dot{m}_{in} - \dot{m}_{out}) & \text{for} \quad \bar{V} = 1 \end{cases} \tag{3}$$

where $K_m$, $A$, $L$, and $a$ are the resistance coefficient, cross-area of the pipe, length of the pipe, and the speed of sound, respectively.

KARI also analytically studied the valve operation order using Monte-Carlo simulation [118,119]. Cha et al. used a staged change function to four state parameters based on the hyperbolic-tangent from before combustion to after combustion to model the start-up process [120]:

$$f = \frac{1}{2}\left(\tanh K_t(t - t_{ignite}) + 1\right) f_{combustion} + \frac{1}{2}\left(\tanh K_t(t - t_{ignite}) + 1\right) f_{nocombustion} \tag{4}$$

where $K_t$ is the coefficient of state change and $t_{ignite}$ is the ignition time.

Additionally, for the side load problem, Wang, T. S. conducted analytical research using computational fluid dynamics (CFD) with two- and three-dimensional conditions [121,122]. The computational methodology was based on a multidimensional, finite-volume, viscous, chemically reacting, unstructured-grid, and pressure-based computational fluid dynamics formulation and a transient inlet condition [121,122]. They conducted subscale combustion tests on three subscale nozzles to establish the criteria and obtained a useful criterion [122]. Tomita, T. et al. also performed analytical research on the side load using an experimental approach [123].

### *3.2. Analysis of the Trend*

In the previous subsection, we review the status of developing a CPS simulation program. In this subsection, trends in simulation programs are analyzed from two perspectives: the modeling approach and the governing equations types in nonlinear modeling.

#### 3.2.1. Perspective of the Modeling Approach

There are two modeling methods, white box modeling and black box modeling, and each modeling method can be classified into linear and nonlinear modeling methods in simulation modeling [124]. The classification is described below and summarized with references depending on the modeling approach in Table 2.

- Nonlinear modeling: In general, nonlinear modeling of CPS models has been used for simulation and analysis. The physics of propulsion system components are generally described using thermo-fluid-dynamic and mechanical conservation equations. Each component is usually not developed to its full complexity since the most accurate model is not the target. The main input data to the model are propellant tank outlet pressure and temperature, geometric and thermal properties, and valve settings. CPS parameters are initially set using design points determined in preliminary design and critical design. After that, they are upgraded and tuned through estimation through generalized residual sum of squares using data obtained from actual tests.
- Linearized modeling: Linearized modeling is the most common modeling by linearizing a nonlinear thermodynamic model (mostly for design control). The approach is linearized around the design points or previously computed equilibrium points. Generally, after each component of a CPS is linearized based on the equilibrium points, all linearized models are combined. However, sometimes parts of all components, which are nonlinear equations that are hard to describe due to complexity or data lack problems, are linearized and combined with other nonlinear forms to make them simple.
- Linear identification: Some researchers have determined a mathematical model using the data obtained from system-level simulations or actual tests rather than developing a model based on thermodynamic equations. The approach mainly considers each valve opening angle as an input and pressure, temperature, and turbopump speed as

outputs. The approach requires preliminary information about the nonlinearity and bandwidth of the system. The responses point to valve nonlinearity, which can be isolated and removed to identify the main system. Through this work, the equations by linear identification have the transfer-function structure between the $j$th input and the $i$th output as:

$$\mathbf{H}_{ij}(s) = \mathbf{C}_i(s\mathbf{I} - \mathbf{A})^{-1}\mathbf{B}_j \tag{5}$$

where **A**, **B**, and **C** are the standard state-space matrices and s is the Laplace variable. To determine the transfer function $\mathbf{H}(s)$ coefficients, mostly the recursive maximum likelihood method (RML) or least-square method (LS) are used by subtracting the nominal values from the perturbed data after defining the order of the model.

- Nonlinear identification: There are several nonlinear identification approaches, including the Volterra series model, block-structured model, neural network model, NARMAX model, and state-space model [125]. However, in the five models, mostly a CPS is modeled using an artificial neural network (ANN) approach, which is adequate for real-time monitoring, diagnosis, and control. Using the ANN approach to represent a CPS requires training with a database from actual tests to provide the correct output determined by the user.

**Table 2.** Classification of the modeling approach.

| Modeling Approach | Types | Refs. (Selected) |
|---|---|---|
| Nonlinear modeling | LPRE | [16,34,39,40,53,57,60,61,67] |
| | SPRM | [77–79,84,87] |
| | HPRM | [96,98–100] |
| Linearized modeling | LPRE | [55,126,127] |
| | SPRM | [128] |
| | HPRM | [97,129,130] |
| Linear identification | LPRE | [131–133] |
| | SPRM | [134] |
| | HPRM | [105,111] |
| Neural network approach | LPRE | [135,136] |
| | SPRM | [137,138] |
| | HPRM | [139,140] |

### 3.2.2. Perspective of Pipe Modeling Method

In the transient state, especially the start-up process, the nonlinear modeling of the CPS requires nonlinear mass flow (mostly water hammer phenomenon) and heat transfer characteristics (if the CPS has a cooling system), so proper analysis and determining how to model the pipe, which is affected by the nonlinear mass flow rate and heat transfer, become more critical. Therefore, to develop dynamic simulation modeling for a CPS, especially an LPRE, three hydrodynamic modeling methods have been used for modeling the nonlinear mass flow in the pipeline: lumped model method, method of characteristics, and volume-junction method (or called lumped parameter method, LPM). The classification is summarized with references depending on the pipe modeling method in Table 3.

The lumped model method is only one dynamic equation for each component of the CPS, so only one ordinary differential equation (ODE) is used for the dynamics of mass flow rate in a pipe, considered a zero-dimensional model [34,60]. In this method, it is essential to determine the time step for solving an ODE, which is smaller than the characteristic time of the CPS component dynamics.

The method of characteristics is a technique for solving the following two partial differential equations:

$$\frac{\partial P}{\partial t} + \frac{1}{A}\rho a_v^2 \frac{\partial Q}{\partial x} = 0 \tag{6}$$

$$\frac{1}{A}\frac{\partial Q}{\partial t}+\frac{1}{\rho}\frac{\partial P}{\partial t}+a_v\sin\theta+\frac{1}{A^2}\frac{f}{2D}Q|Q|=0 \tag{7}$$

where $A$, $D$, and $f$, are the area, diameter, and friction factor of the pipeline, respectively, $\rho$ is the density of the fluid, and $a_v \sin\theta$ is the vehicle acceleration component along the line axis.

The PDEs should be solved because the transient state fluid flow is unsteady in a pipe of CPSs, especially in the start-up process [37,141]. However, since there is no general solution for PDEs, the PDEs can be transformed by the method of characteristics, which is an application of a lagrangian multiplier method using the two PDEs, to two sets of two ordinary differential equations in a two-dimensional (pipeline and time axises) plane, as shown in Figure 9. Using the technique, fluid properties can be obtained by pipeline ($x$-axis) and time ($t$-axis) in the two-dimensional grid with two characteristic lines ($C_p$ and $C_m$).

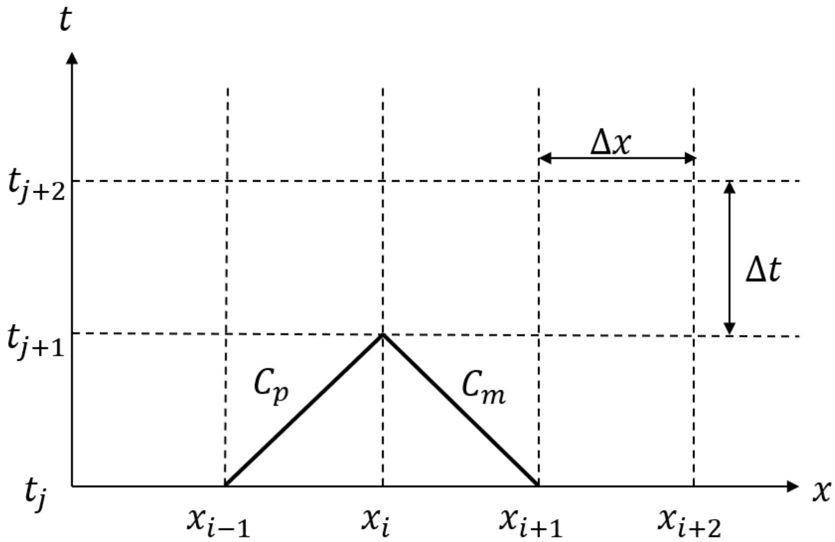


**Figure 9.** Characteristics of the x-t plane [37].

Finally, the volume-junction method (or LPM) is similar to the node-link method used in other flow network analysis codes, as shown in Figure 10 [29,39]. In this method, the number of volumes (or lumps) and the location of each are significant. Examining the system frequencies is required when determining the number of volumes (or lumps). Furthermore, since the discretization of a system is often determined by the geometrical constraints of the system being simulated, fixing the system frequency range is considered [39].

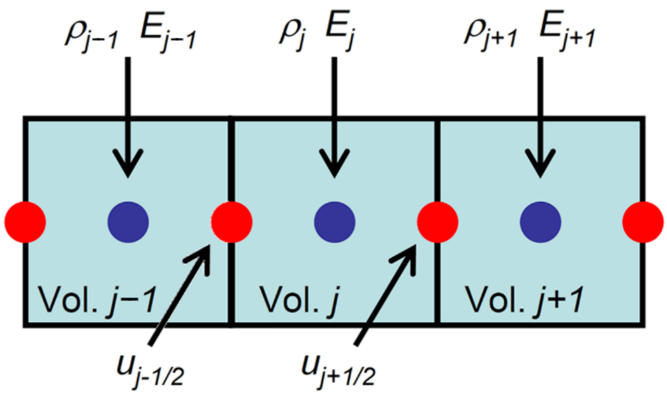


**Figure 10.** Schematic of the volume-junction method [29].

**Table 3.** The classification of the method.

| Method | Refs. (Selected) |
|---|---|
| Lumped model method | [34,40,60,67] |
| Method of characteristics | [37,141] |
| Volume-junction method (Lumped parameter method) | [29,39,47,142] |

### 3.2.3. Others

In addition to the ones mentioned above, there are other trends, the most representative of which is the module approach. The security concerns make acquiring experimental data and developing full simulation models difficult. However, once a CPS simulation program based on modules is developed, it becomes easy for some research groups to develop and upgrade new models simply by upgrading each component module. Therefore, the module-based simulation approach has become a trend because of its usefulness, so many countries and institutes have tried to create and use module-based simulation programs, as summarized in Table 4 (mostly for LPRE). Then, by applying the program, mainly developed focusing on LPREs, researchers can develop other CPSs, including SPRMs and HPRMs [112,113]. The Ecosimpro and ESPSS of ESA, the representative module program, can be organized in Table 5 and simulated as shown in Figure 11.

**Table 4.** The module-based simulation program of each country and institute.

| Country | Institute | Simulation Toolbox | Refs. (Selected) |
|---|---|---|---|
| U.S. | NASA | ROCETS | [28] |
| Europe | ESA | EcosimPro + ESPSS | [31,32] |
| China | NUDT | LRETMMSS | [47] |
| China | HUST | Self-developed Toolbox (Modelica) | [48] |
| China | BUAA | Self-developed Toolbox (MATLAB) | [52] |
| Iran | KNTU | Self-developed Toolbox (MATLAB) | [52] |
| Korea | KAU | Self-developed Toolbox (MATLAB) | [61,62] |

**Table 5.** The category of EcosimPro+ESPSS [143,144].

| Main Category | Subcategory | Subsubcategory |
|---|---|---|
| Fluid Properties | - | Ideal gas, Simplified liquids, Real fluids |
| Fluid Flow 1D | AbstracJunction | Jun_TMD, DeadEnd, Filter |
| | Time dependent Boundaries | VolPT_TMD, VolPx_TMD, VolTx_TMD |
| | Cavities | Chamber, Volume1, Volume2, Volume5 |
| | AbstacJunctionLoss | Juntion, ValveCheck, Valve, ValvePressRegDown, VallvePressRegUp, ValveCheck_Dynamic, VolPsTsVs_TMD |
| | Sensor | SensorJun, SensorPipe, SensorVol |
| | Channel | Pipe, Tube, Pipe_res, Pipe_Rect, Tube_Rect |
| | Etc. | WorkingFluid, VTee, WorkingFluuid, HeatExchanger, Nozzle, ColdThruster |
| Tanks | Propellent Tank | Tank_single, Tank_Sphere, Cylinder_ins, Sphere_ins, Tank_CylDomes, Dome_ins, Tank_Bladder, Tank_CylDomesSph |
| Combustion Chambers | Combustor | ABS-Combustor_eq, ABS−Combustor_rate |
| | Preburner | PreBurnerCoat_eq, PreBurner_eq, PreBurner_rate, reBurnerCoat_rate |
| | Nozzle | Nozzle, Nozzle_Ex, Nozzle_Ex2 |
| | CobustChamber_Nozzle | CombustChamberNozzle_eq, CombustChambbeerNozzleCoat_eq, CombustChamberNozzle_rate, CombustChambberNozzleCoat_rate |
| | Cooling Jacket | CoolingJacket, CoolingJacket_simple, CoolingJacket_tore |
| | Injector | - |
| Turbo Machinery | Compressor | Compressor, Compressor_gen |
| | Pump | Pump, Pump_gen, Pump_vaccum |
| | Turbine | Turbine, Turbine_gen |

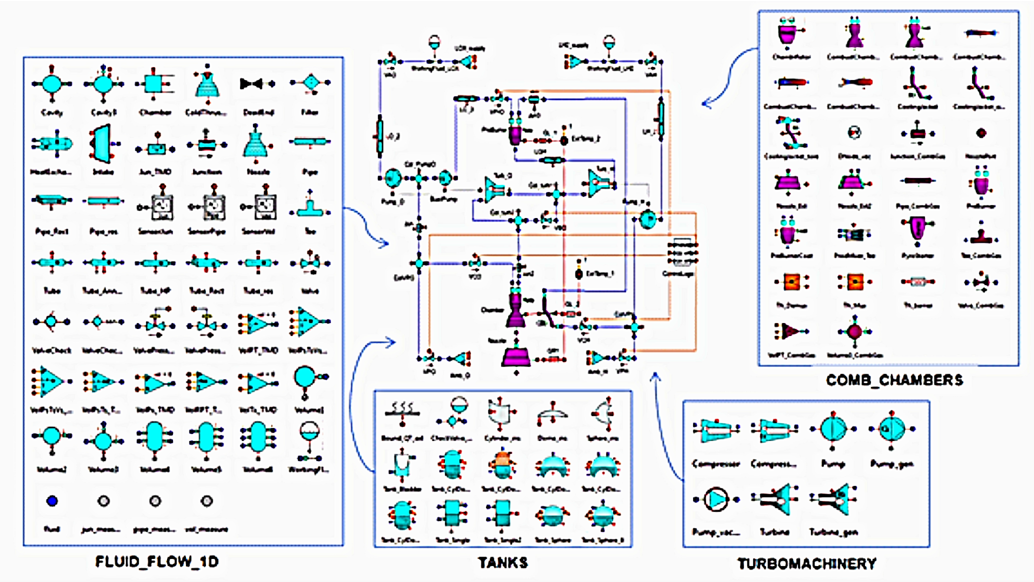


**Figure 11.** Interface and library components of EcosimPro and ESPSS [145].

## 4. Fundamental Mathematical Modeling Approach

As mentioned above, there are four major approaches to simulation modeling, and the nonlinear modeling approach is a fundamental approach based on the laws of physics above all else. The approach requires deriving dynamic equations that represent the dynamics of CPSs in the form of differential and algebraic Equations (DAEs). In DAEs, the differential equations are derived from seven governing equations, and algebraic equations are derived from empirical equations or laws of thermal-fluid dynamics.

This section summarizes and organizes dynamic equations for a nonlinear modeling approach. For this, we classify into three groups: governing equations (component dynamics), algebraic equations or phenomenological equations (physical laws), and characteristics equations (empirical equations or lookup tables from experiment data).

### *4.1. Governing Equations*

A CPS consists of only a combustion chamber at least and a supply, propulsion, and piping system at most. The dynamics of these systems can be expressed using several dynamic equations composed of first-order ODEs, which can be derived from seven governing Equations [34].

#### 4.1.1. Rotational Dynamics

The rotational dynamics for a turbopump or electric pump in a CPS can be represented as:

$$I_p \frac{d}{dt}\omega = \tau_{in} - \tau_{out} \tag{8}$$

where $I_p$ is the moment of inertia of the pump rotor, $\tau_{in}$ is the torque produced by the turbine or electrical motor, $\tau_{out}$ is the torque absorbed by the pump, and $\omega$ is the angular velocity.

#### 4.1.2. Mass Flow Rate

This equation is for a mass flow rate in a pipe by applying Newton's second law. Since the pipe has friction and resistance elements, the overall pressure drop occurs according to the fluid density, speed, and pipe characteristics, so the dynamics can be expressed as follows:

$$\left(\frac{L}{A}\right)\frac{d}{dt}\dot{m} = P_{in} - P_{out} - K|\dot{m}|\dot{m} \tag{9}$$

where $L$, $A$, and $K$ are the pipe length, cross-area of the pipe, and resistance coefficient, respectively, and $P_{in}$, $P_{out}$, and $\dot{m}$ are the inlet pressure, outlet pressure, and average mass flow rate in the pipe, respectively.

#### 4.1.3. Pressure Dynamics

The fluid pressure can change by mass flow rate difference or property changes. The dynamics can be represented based on the fluid state.

For a liquid state:

$$\kappa(\rho V)\frac{d}{dt}P = \sum \dot{m}_{in} - \sum \dot{m}_{out} \tag{10}$$

$$\kappa = \frac{1}{\rho}\frac{d\rho}{dP} \tag{11}$$

Furthermore, in the case of the gas state, we can assume the fluid is an ideal gas, then:

$$\frac{V}{RT}\frac{d}{dt}P = \sum \dot{m}_{in} - \sum \dot{m}_{out} \tag{12}$$

$$\kappa\rho = \frac{d\rho}{dP} = \frac{1}{RT} \tag{13}$$

where $P$, $\kappa$, $\rho$, $V$, $R$, and $T$ are the pressure, fluid compressibility, density, volume, gas constant, and temperature, respectively, and $\dot{m}_{in}$ and $\dot{m}_{out}$ are the inlet and outlet mass flow rates, respectively.

#### 4.1.4. Density Equation

Some fluids are more sensitive to density changes than pressure changes, especially when dealing with heat exchangers using cryogenic propellants. This type of dynamics is fundamentally the same as fluid capacitance dynamics, considering that the volume is invariant:

$$V\frac{d}{dt}\rho = \sum \dot{m}_{in} - \sum \dot{m}_{out} \tag{14}$$

#### 4.1.5. Energy Balance in Heat Exchangers

An essential part of CPRS (primarily for LPREs) dynamics is dealing with the change in the properties of fluids used in the heat transfer process in a heat exchanger, especially with cryogenic propellants. Let us focus on the coolant fluid inside the space between the walls. Since the coolant does not perform any mechanical work, a simple heat flow balance for the fluid between the wall gives:

$$\rho V\frac{d}{dt}u = \dot{Q}_{w,in} - \dot{Q}_{w,out} + (\dot{m}h)_{in} - (\dot{m}h)_{out} \tag{15}$$

where $\dot{Q}_w$, $u$, and $h$ are the heat flow rate between the walls and the coolant fluid, internal energy, and enthalpy of the fluid, respectively.

#### 4.1.6. Heat Transfer Equations

In a heat exchanger, the fluid temperature changes by the metal walls of the system. Assuming that the volume change is negligible to make the network to zero according to the first law of thermodynamics, the average transient hot wall temperature as:

$$\frac{d}{dt}T_w = \frac{1}{mc_v}\left(\dot{Q}_{c,in} - \dot{Q}_{w,in}\right) \tag{16}$$

where $m$ is the mass of the wall, $c_v$ is the specific heat of the wall material, and $\dot{Q}_c$ is the heat flow rate between the hot fluid and the walls.

4.1.7. Time Delay Equation

Some variables used in the dynamic model for a CPS do not have an instantaneous physical response to changes in the state of other variables, such as a combustion process. This delay can be expressed using a first-order time lag as:

$$\frac{d}{dt}\dot{m}(t) = \frac{1}{\epsilon}(\dot{m}(t+\epsilon) - \dot{m}(t)) \tag{17}$$

where $\epsilon$ is the amount of the time delay.

*4.2. Algebraic Equations*

In the dynamics of a CPS, algebraic Equations (AEs), also called phenomenological equations, are needed to link each variable in ODEs based on thermodynamic theory and equilibrium relationships. For this, we summarize and organize the representative algebraic equations in this subsection.

4.2.1. The Combustion Gas Mass Flow Rate

The mass flow rate of combustion gas ($\dot{m}_c$) through the nozzle throat area can be expressed as:

$$\dot{m}_c = C_d P_c A_n \sqrt{\frac{k_c}{R_c T_c}\left(\frac{2}{k_c+1}\right)^{\frac{k_c+1}{k_c-1}}} \tag{18}$$

where $C_d$, $A_n$, $P_c$, $k_c$, $R_c$, and $T_c$ are the discharge coefficient, nozzle throat area, pressure, heat specific ratio, gas constant, and temperature of the combustion gas, respectively.

4.2.2. Injector Pressure Decremental Equation

An injector pressure decrement ($\Delta P_i$) can be described as follows by assuming that there is no flow loss and no change with time (the time delay phenomenon can be considered in the time delay equation):

$$\Delta P_i = -K_i \dot{m}_i^2 \tag{19}$$

where $K_i$ and $\dot{m}_i$ are injector resistance coefficient and mass flow rate, respectively.

4.2.3. The Power or Torque of the Pump

The performance of a pump can be described in terms of the power ($W_p$) or torque ($\tau_p$) consumed as:

$$W_p = \frac{\dot{m}_p \Delta P_p}{\eta \rho} \quad \text{or} \quad \tau_p = \frac{\dot{m}_p \Delta P_p}{\omega \eta \rho} \tag{20}$$

where $\dot{m}_p$, $\Delta P_p$, and $\eta_p$ are mass flow rate, pressure increment in the pump, and pump efficiency, respectively.

4.2.4. The Power or Torque of the Turbine and Motor

A gas turbine is widely used to generate the power or torque for the pump, especially large-thrust LPREs. Unlike the pump, the power ($W_t$) or torque ($\tau_t$) of a turbine can be obtained as follows in proportion to the specific heat ratio and efficiency of combustion gas, inlet flow rate, and inlet/outlet pressure ratio:

$$W_t = \dot{m}_t \eta_t \frac{k_t}{k_t-1} R_t T_t \left(1 - \frac{P_{ti}}{P_{te}}\right)^{\frac{k_t-1}{k_t}} \quad \text{or} \quad \tau_t = \frac{1}{\omega}\dot{m}_t \eta_t \frac{k_t}{k_t-1} R_t T_t \left(1 - \frac{P_{ti}}{P_{te}}\right)^{\frac{k_t-1}{k_t}} \tag{21}$$

where $\dot{m}_t$, $\eta_t$, $P_{ti}$, and $P_{te}$ are the mass flow rate in the turbine, turbine efficiency, turbine inlet pressure, and turbine outlet pressure, respectively.

In the case of using an electrical motor to generate power or torque, especially low-thrust LPREs or large-thrust HPRMs, the motor torque ($\tau_m$) can be described as:

$$\tau_m = i_m C_{mt} \tag{22}$$

where $C_{mt}$ is the torque coefficient of the motor and $i_m$ is the current of the motor, which is a state variable of the motor dynamics and can be controlled by the voltage [146].

*4.3. Characteristics Equations*

In the simulation modeling process, some dynamics are difficult to express or obtain dynamic equations for due to the complexity of dynamics or the dynamics that have not yet been accurately identified theoretically. For this, empirical equations or lookup tables from experiment data are needed.

4.3.1. Pump Pressure Incremental Equation

For a pump pressure increment ($\Delta P_p$), characteristic curves are often used to define the pump performance over a range of volumetric flow rates and rotational speeds [147]. These curves can be analytically defined as:

$$\Delta P_p = A_{pp}\omega^2 + B_{pp}\omega \dot{m}_p + C_{pp}\dot{m}_p^2 \tag{23}$$

where $A_{pp}$, $B_{pp}$, and $C_{pp}$ are coefficients of the pump, which can be determined by the characteristic curves, and $\omega$ and $\dot{m}_p$ are pump rotational velocity and the mass flow rate in the pump, respectively.

4.3.2. Propellant State Equation

Since there are many types of propellants and a CPS operates in a wide range of temperature and pressure, data on various propellant properties in a wide temperature and pressure range are also required to design and analyze the performance of a CPS. The properties have been mostly expressed in an empirical equation, such as burn rate for a solid propellant or surrogate mixture model for liquid propellant from previous studies, or a dataset or lookup table using data from Chemical Equilibrium with Application (CEA) or the National Institute of Standards and Technology (NIST) [148–157].

A general empirical equation of the burn rate of solid propellants used in SPRMs or HPRMs [19] can be represented as:

$$\frac{d}{dt} r_b = a_p P_c^n \tag{24}$$

where $a_p$ and $n$ are an empirical constant and burning rate exponent, respectively.

Furthermore, as the solid propellant burns, the volume of combustion chamber space increases, so by assuming the volume change is related only to the solid propellant surface movement due to the propellant burning, it can be expressed as:

$$\frac{d}{dt} V_c = r_b A_b \tag{25}$$

where $A_b$ is the burning surface area of the solid propellant.

In the combustion process, the properties of the combustion gases change rapidly and depend on many factors, making it difficult to determine their properties. To simplify this, many researchers have created a dataset using data obtained from self-experiments or CEA or NIST, and used the dataset to develop input/output functions such as lookup tables. Based on the empirical experience, the function of the combustion gas properties generally can be represented by the function of the oxidizer-to-fuel-mixture ratio and combustion pressure:

$$T_c = f_c(\mathrm{OF}_c, P_c) \tag{26}$$

$$R_c = f_c(\mathrm{OF}_c, P_c) \tag{27}$$

$$k_c = f_c(\mathrm{OF}_c, P_c) \tag{28}$$

### *4.4. Mathematical Modeling of Chemical Propulsion Systems*

Various simulation modelings of CPSs have been developed by the nonlinear approach using these dynamic equations. In this section, we summarize the required dynamic equations depending on a CPS and organize them in Table 6.

SPRMs have a simple structure among three types of CPSs, as mentioned in Ref. [19], so the dynamic simulation of the solid propulsion system is also simple. In the seven governing equations, the simulation can be represented only using one governing equation: the pressure equation for an SPRM [72]. However, to represent the simulation performance more accurately, considering the volume changes in the combustion chamber of an SPRM is also needed [77]. Furthermore, if a simulation model is more precise than required, some researchers also consider the density of combustion gas. The density change equation is not essential, but for a controllable thrust solid propulsion system using a special nozzle like a pintle nozzle, the combustion gas density dynamics can be an influential element because the moving pintle changes the nozzle throat area and it directly affects the combustion gas density [78,82,84]. Therefore, an SPRM simulation program can be developed using two or three governing equations.

LPREs have the most complex structure among the three types of CPSs, so the dynamic simulation of an LPRE is also complicated. In the seven governing equations, the simulation can be represented using all or four equations depending on the fuel type: cryogenic or not. In an LPRE, since the cooling system (or heat exchanger) uses fuel before injecting it into the combustion chamber, the heat from the combustion gas changes the fuel state, such as gasified or two-phase flow. For this reason, if the fuel is a cryogenic propellant, the fuel state changes intensify, so the nonlinearity of the pressure drop by the heat becomes more extreme than in other types of fuels [29,34,53,158,159]. On the other hand, if the fuel is not cryogenic, the nonlinearity of the pressure drop by the heat is negligible enough to represent using the function of mass flow rate with a constant coefficient, so the governing equations related to the heat exchangers can become algebraic equations and the differential type equations are required no more. In that case, only four governing Equations (Rotational dynamics, Mass flow rate, Pressure dynamics, and Time delay dynamics) are required to represent the liquid propulsion system simulation system [39,40,60].

HPRMs are the combined characteristics of a liquid and solid propulsion system, so the complexity of the dynamic simulation is also between SPRMs and LPREs. In the seven governing equations, the simulation can be represented using three or four equations depending on the size of an HPRM. For the small thrust size of an HPRM, a gas-pressurized system is enough to feed the oxidizer or fuel to the combustion chamber, which is filled with solid fuel or oxidizer [100,106,109,110]. However, in the case of large thrust and deep throttling, there is a limit to using the gas pressure method, so a pump is required [160,161]. For this reason, the three or four governing equations are needed depending on the size of the system. Furthermore, since the hybrid propulsion system also has the characteristics of the solid propulsion system, the equation related to the volume changes in the combustion chamber is also needed.

**Table 6.** The classification of the modeling.

| Model of CPS | Characteristics (Perspective of ODEs) |
| --- | --- |
| SPRM | • Pressure dynamics<br>• Volume change dynamics (if more accurate)<br>• Density equation (if more accurate) |
| HPRM | • Pressure dynamics<br>• Mass flow rate<br>• Time delay dynamics<br>• Rotational dynamics (depending on thrust)<br>• Volume change dynamics (if more accurate) |
| LPRE | • Rotational dynamics<br>• Mass flow rate<br>• Pressure dynamics<br>• Time delay dynamics<br>• Density equation (depending on fuel types)<br>• Energy balance in heat exchanger (depending on fuel types)<br>• Heat transfer equation (depending on fuel types) |

## 5. Conclusions

This study included a comprehensive review of the mathematical modeling of chemical propulsion systems (CPSs) and summarized the simulation modeling approaches and fundamental mathematical dynamic equations categorized based on types of equations and CPSs, respectively. The simulation modeling approach has changed from a total system to each component of a CPS via the modularization method. In turn, the main development body has changed from a single developer monopolizing a whole CPS experimental data to a collaboration of many different institutes specialized in each component to develop and upgrade a module focusing on the component and organize a library-type integrated program combining each module. These days, as a new space age has started, an accurate and reliable simulation modeling approach is urgently needed to develop a low-cost commercialization space launch vehicle (SLV) and a reliable maintenance process for a reusable launch vehicle (RLV). Furthermore, supposing a simulation model that can be carried onboard is developed, it can be used for predicting the potential failures using the actual flight data and monitoring the condition of the vehicle in real-time. Based on the advantages of accurate and reliable system-level simulation modeling of a CPS, the control system design for a SLV or RLV can be completed very well, and it will guarantee the mission capability. Therefore, the development of a CPS simulation modeling will generate enormous profits, which is why a simulation system of a CPS.

**Author Contributions:** Conceptualization, J.C.; methodology, J.C.; validation, J.C.; formal analysis, J.C.; investigation, J.C.; resources, J.C.; writing—original draft preparation, J.C.; writing—review and editing, J.C.; visualization, J.C.; supervision, J.C.; project administration, J.C.; funding acquisition, J.C. All authors have read and agreed to the published version of the manuscript.

**Funding:** This research received European Regional Development Fund in Kiruna, Sweden.

**Data Availability Statement:** Not applicable

**Conflicts of Interest:** The authors declare no conflict of interest.

## Abbreviations

The following abbreviations are used in this manuscript:

| | |
| --- | --- |
| $A$ | Cross-area of pipe |
| $A_b$ | Burning surface area of solid propellant |
| $A_n$ | Nozzle throat area |
| $A_{pp}$, $B_{pp}$, $C_{pp}$ | Coefficients of pump |
| $C_d$ | Discharge coefficient |
| $C_{mt}$ | Torque coefficient of motor |
| $D$ | Diameter of pipe |
| $I_p$ | Moment of inertia of pump rotor |

| | |
|---|---|
| $K$ | Resistance coefficient of pipe |
| $K_i$ | Injector resistance coefficient |
| $K_m$ | Resistance coefficient |
| $K_t$ | Coefficient of state change |
| $L$ | Length of pipe |
| $\mathrm{OF}_c$ | Oxidizer to fuel mixture ratio |
| $P$ | Pressure |
| $P_c$ | Combustion chamber pressure |
| $P_{in}$ | Inlet pressure |
| $P_{out}$ | Outlet pressure |
| $P_{te}$ | Turbine outlet pressure |
| $P_{ti}$ | Turbine inlet pressure |
| $\Delta P_i$ | Injector pressure decrement |
| $\Delta P_p$ | Pump pressure increment |
| $Q$ | Flow rate |
| $\dot{Q}_w$ | Heat flow rate between the walls and the coolant fluid |
| $\dot{Q}_c$ | Heat flow rate between the hot fluid and the wall |
| $R$ | Gas constant |
| $R_c$ | Gas constant of combustion gas |
| $T$ | Temperature |
| $T_c$ | Temperature of combustion gas |
| $T_w$ | Hot wall temperature |
| $V$ | Volume |
| $V_c$ | Volume of combustion chamber |
| $W_p$ | Power of pump |
| $W_t$ | Power of turbine |
| $\bar{V}$ | Pipe volume ratio of total and filled |
| $a$ | Speed of sound |
| $a_p$ | Empirical constant |
| $a_v$ | Acceleration of vehicle |
| $c_v$ | Specific heat of the wall material |
| $f$ | Friction factor of pipeline |
| $h$ | Enthalpy of fluid |
| $i_m$ | Current of motor |
| $k_c$ | Heat specific ratio of combustion gas |
| $m$ | Mass of the wall |
| $\dot{m}$ | Mass flow rate in pipe |
| $\dot{m}_c$ | Combustion gas mass flow rate |
| $\dot{m}_i$ | Injector mass flow rate |
| $\dot{m}_{in}$ | Inlet mass flow rate |
| $\dot{m}_{out}$ | Outlet mass flow rate |
| $\dot{m}_p$ | Mass flow rate in pump |
| $\dot{m}_t$ | Mass flow rate in turbine |
| $n$ | Burning rate exponent |
| $r_b$ | Burning rate |
| $t_{ignite}$ | Ignition time |
| $u$ | Internal energy of fluid |
| $\epsilon$ | Amount of the time delay |
| $\eta_p$ | Pump efficiency |
| $\eta_t$ | Turbine efficiency |
| $\kappa$ | Fluid compressibility |
| $\rho$ | Density of fluid |
| $\tau_{in}$ | Torque produced by turbine or motor |
| $\tau_m$ | Torque of motor |
| $\tau_{out}$ | Torque absorbed by pump |
| $\tau_p$ | Torque of pump |
| $\tau_t$ | Torque of turbine |
| $\omega$ | Angular velocity of pump |

## References


1. Muelhaupt, T.J.; Sorge, M.E.; Morin, J.; Wilson, R.S. Space traffic management in the new space era. *J. Space Saf. Eng.* **2019**, *6*, 80–87. [CrossRef]
2. Kuntanapreeda, S.; Hess, D. Opening access to space by maximizing utilization of 3D printing in launch vehicle design and production. *Appl. Sci. Eng. Prog.* **2021**, *14*, 143–145. [CrossRef]
3. Wekerle, T.; Pessoa, J.B.; Costa, L.E.V.L.d.; Trabasso, L.G. Status and trends of smallsats and their launch vehicles—An up-to-date review. *J. Aerosp. Technol. Manag.* **2017**, *9*, 269–286. [CrossRef]
4. Jones, H. The recent large reduction in space launch cost. In Proceedings of the 48th International Conference on Environmental Systems, Albuquerque, NM, USA, 8–12 July 2018.
5. Kim, C.T.; Yang, I.; Lee, K.; Lee, Y. Technology Development Prospects and Direction of Reusable Launch Vehicles and Future Propulsion Systems. *J. Korean Soc. Aeronaut. Space Sci.* **2016**, *44*, 686–694.
6. Choo, K.; Mun, H.; Nam, S.; Cha, J.; Ko, S. A survey on recovery technology for reusable space launch vehicle. *J. Korean Soc. Propuls. Eng.* **2018**, *22*, 138–151. [CrossRef]
7. Kim, C.; Lim, B.; Lee, K.; Park, J. A Study on Fuel Selection for Next-Generation Launch Vehicles. *J. Korean Soc. Propuls. Eng.* **2021**, *25*, 62–80. [CrossRef]
8. Bae, J.; Koo, J.; Yoon, Y. Development trend of low cost space launch vehicle and consideration of next generation fuel. *J. Korean Soc. Aeronaut. Space Sci.* **2017**, *45*, 855–862. [CrossRef]
9. Schmierer, C.; Kobald, M.; Tomilin, K.; Fischer, U.; Schlechtriem, S. Low cost small-satellite access to space using hybrid rocket propulsion. *Acta Astronaut.* **2019**, *159*, 578–583. [CrossRef]
10. Yu, B.; Kwak, H.D.; Kim, H.J. Effects of the O/F Ratio on the Performance of a Low Thrust LO X/Methane Rocket Engine with an ElecPump-fed Cycle. *Int. J. Aeronaut. Space Sci.* **2020**, *21*, 1037–1046. [CrossRef]
11. Kawatsu, K.; Tsutsumi, S.; Hirabayashi, M.; Sato, D. Model-based fault diagnostics in an electromechanical actuator of reusable liquid rocket engine. In Proceedings of the AIAA Scitech 2020 Forum, Orlando, FL, USA, 6–10 January 2020; p. 1624.
12. Satoh, D.; Tsutsumi, S.; Hirabayashi, M.; Kawatsu, K.; Kimura, T. Estimating model parameters of liquid rocket engine simulator using data assimilation. *Acta Astronaut.* **2020**, *177*, 373–385. [CrossRef]
13. Cha, J.; Ha, C.; Ko, S. A survey on health monitoring and management technology for liquid rocket engines. *J. Korean Soc. Propuls. Eng.* **2014**, *18*, 50–58. [CrossRef]
14. Cha, J.; Ha, C.; Koo, J.; Ko, S. Dynamic simulation and analysis of the space shuttle main engine with artificially injected faults. *Int. J. Aeronaut. Space Sci.* **2016**, *17*, 535–550. [CrossRef]
15. Lee, K.; Cha, J.; Ko, S. A Survey on Fault Detection and Diagnosis Method for Open-Cycle Liquid Rocket Engines through China R&D Case. *J. Aerosp. Syst. Eng.* **2017**, *11*, 22–30.
16. Cha, J. Transient State Modeling, Simulation, and Fault Detection/Diagnosis of an open-cycle Liquid Rocket Engine. Ph.D. Thesis, Department of Aerospace and Mechanical Engineering, Republic of Korea Aerospace University, Goyang, Republic of Korea, 2019.
17. Lee, J.; Cha, S.W.; Ha, D.; Kee, W.; Lee, J.; Huh, H.; Roh, T.S.; Lee, H.J. Research trend analysis on modeling and simulation of liquid propellant supply system. *J. Korean Soc. Propuls. Eng.* **2019**, *23*, 39–50. [CrossRef]
18. Wang, T.; Ding, L.; Yu, H. Research and development of fault diagnosis methods for liquid rocket engines. *Aerospace* **2022**, *9*, 481. [CrossRef]
19. Sutton, G.P.; Biblarz, O. *Rocket Propulsion Elements*; John Wiley & Sons: Hoboken, NJ, USA, 2016.
20. Humble, R.W.; Gary, H.N.; Larson, W.J. *Space Propulsion Analysis and Design*; McGraw-Hill Companies: New York, NY, USA, 1995.
21. Taylor, T.S. *Introduction to Rocket Science and Engineering*; CRC Press: Boca Raton, FL, USA, 2017.
22. El-Sayed, A.F. *Fundamentals of Aircraft and Rocket Propulsion*; Springer: Berlin/Heidelberg, Germany, 2016.
23. Huzel, D.K. *Modern Engineering for Design of Liquid-Propellant Rocket Engines*; AIAA: Reston, VA, USA, 1992; Volume 147.
24. Davenas, A. *Solid Rocket Propulsion Technology*; Pergamon Press: Oxford, UK, 2012.
25. Kuo, K.K.; Chiaverini, M.J. *Fundamentals of Hybrid Rocket Combustion and Propulsion*; American Institute of Aeronautics and Astronautics: Reston, VA, USA, 2007.
26. Kalnin, V.; Sherstiannikov, V. Hydrodynamic modelling of the starting process in liquid-propellant engines. *Acta Astronaut.* **1981**, *8*, 231–242. [CrossRef]
27. Harland, D.M.; Lorenz, R. *Space Systems Failures: Disasters and Rescues of Satellites, Rocket and Space Probes*; Springer Science & Business Media: Berlin/Heidelberg, Germany, 2007.
28. Mason, J.; Southwick, R. *Large Liquid Rocket Engine Transient Performance Simulation System*; Technical Report; The National Aeronautics and Space Administration: Huntsville, AL, USA, 1991.
29. Yamanishi, N.; Kimura, T.; Takahashi, M.; Okita, K.; Atsumi, M.; Negishi, H. Transient analysis of the LE-7A rocket engine using the rocket engine dynamic simulator (REDS). In Proceedings of the 40th AIAA/ASME/SAE/ASEE Joint Propulsion Conference and Exhibit, Fort Lauderdale, FL, USA, 11–14 July 2004; p. 3850.
30. Francesco, D.M. Modelling and Simulation of Liquid Rocket Engine Ignition Transients. Ph.D. Thesis, Department of Aeronautics and Space Engineering, Sapienza University of Rome, Roma, Italy, 2011.
31. Moral, J.; Pérez Vara, R.; Steelant, J.; De Rosa, M. ESPSS Simulation Platform. In Proceedings of the Space Propulsion 2010, San Sebastian, Spain, 3–6 May 2010.

32. Moral, J.; Rodríguez, F.; Vilá, J.; Di Matteo, F.; Steelant, J. 1-D Simulation of Solid and Hybrid Combustors with EcosimPro/ESPSS. In Proceedings of the Space Propulsion 2014, Cologne, Germany, 19–22 May 2014; pp. 19–22.
33. Unit, H.S.A.; Unit, S.D. *Engine Balance and Dynamics Model*; Technical Report; Report Number RL00001; Rockwell International Corporation, Rocket Dyne Division: Oshkosh, WI, USA, 1992.
34. Lozano-Tovar, P.C. Dynamic Models for Liquid Rocket Engines with Health Monitoring Application. Master's Thesis, Department of Aeronautics and Astronautics, Massachusetts Institute of Technology, Cambridge, MA, USA, 1998.
35. Ho, N.T. Failure Detection and Isolation for the Space Shuttle Main Engine. Master's Thesis, Department of Mechanical Engineering, Massachusetts Institute of Technology, Cambridge, MA, USA, 1998.
36. Ho, N.; Lozano, P.; Martinez-Sanchez, M.; Mangoubi, R.; Ho, N.; Lozano, P.; Martinez-Sanchez, M.; Mangoubi, R. Failure detection and isolation for the Space Shuttle Main Engine. In Proceedings of the 33rd Joint Propulsion Conference and Exhibit, Seattle, WA, USA, 6–9 July 1997; p. 2821.
37. Ruth, E.; Ahn, H.; Baker, R.; Brosmer, M. Advanced liquid rocket engine transient model. In Proceedings of the 26th Joint Propulsion Conference, Orlando, FL, USA, 16–18 July 1990; p. 2299.
38. Manfletti, C. Start-Up Transient Simulation of a Pressure Fed LOx/LH2 Upper Stage Engine Using the Lumped Parameter-based MOLIERE Code. In Proceedings of the 46th Joint Propulsion Conference & Exhibit, Nashville, TN, USA, 25–28 July 2010.
39. Manfletti, C. Transient Behaviour Modeling of Liquid Rocket Engine Components. Ph.D. Thesis, Aerospace, Aeronautical and Astronautical/Space Engineering, RWTH Aachen University, Aachen, German, 2010.
40. Pérez-Roca, S.; Marzat, J.; Piet-Lahanier, H.; Langlois, N.; Galeotta, M.; Farago, F.; Le Gonidec, S. Model-based robust transient control of reusable liquid-propellant rocket engines. *IEEE Trans. Aerosp. Electron. Syst.* **2020**, *57*, 129–144. [CrossRef]
41. Pérez-Roca, S. Model-based Robust Transient Control of Reusable Liquid-Propellant Rocket Engines Transient Behaviour Modeling of Liquid Rocket Engine Components. Ph.D. Thesis, University of Paris-Saclay, Paris, France, 2020.
42. Lebedinsky, E.; Mosolov, S.; Kalmykov, G.; Zenin, E.; Tararyshkin, V.; Fedotchev, V. *Computer Models of Liquid-Propellant Rocket Engines*; Mashinostroenie: Moscow, Russia, 2009.
43. Belyaev, E.; Chvanov, V.; Chervakov, V. *Mathematical Modeling Workflow Liquid Rocket Engines*; Moscow Aviation Institution: Moscow, Russia, 1999.
44. Wu, J.; Zhang, Y.; Chen, Q. Transient performance simulation of a large liquid rocket engine under fault conditions. *J. Aerosp. Power China* **1994**, *9*, 361–365.
45. Wu, J.; Zhang, Y.; Chen, Q. Steady fault simulation and analysis of liquid rocket engine. *J. Propuls. Technol. China* **1994**, *15*, 6–13.
46. Zhang, Y.; Wu, J.; Huang, M.; Zhu, H.; Chen, Q. Liquid-propellant rocket engine health-monitoring techniques. *J. Propuls. Power* **1998**, *14*, 657–663. [CrossRef]
47. Liu, K.; Zhang, Y. A study on versatile simulation of liquid propellant rocket engine systems transients. In Proceedings of the 36th AIAA/ASME/SAE/ASEE Joint Propulsion Conference and Exhibit, Huntsville, AL, USA, 17–19 July 2000; p. 3771.
48. Wei, L.; Liping, C.; Gang, X.; Ji, D.; Haiming, Z.; Hao, Y. Modeling and simulation of liquid propellant rocket engine transient performance using modelica. In Proceedings of the 11th International Modelica Conference, Versailles, France, 21–23 September 2015; pp. 485–490.
49. Zheng, Y.; Tong, X.; Cai, G.; Chen, J. Simulation and optimization of liquid propellants rocket engine for system design. *J. Beijing Univ. Aeronaut. Astronaut.* **2006**, *32*, 40–45.
50. Zhu, S. *H2/O2 Rocket Engine and Cryogenic Technique*; National Defense Industry Press: Beijing, China, 1995; pp. 15–17.
51. Cai, G.; Fang, J.; Zheng, Y.; Tong, X.; Chen, J.; Wang, J. Optimization of system parameters for liquid rocket engines with gas-generator cycles. *J. Propuls. Power* **2010**, *26*, 113–119. [CrossRef]
52. Naderi, M.; Liang, G.; Karimi, H. Modular simulation software development for liquid propellant rocket engines based on MATLAB Simulink. In Proceedings of the MATEC Web of Conferences. EDP Sciences, Beijing, China, 12–14 May 2017; Volume 114, p. 02010.
53. Naderi, M.; Liang, G. Static performance modeling and simulation of the staged combustion cycle LPREs. *Aerosp. Sci. Technol.* **2019**, *86*, 30–46. [CrossRef]
54. Mota, F.A.d.S.; Hinckel, J.N.; Rocco, E.M.; Schlingloff, H. Modeling and analysis of a LOX/Ethanol liquid rocket engine. *J. Aerosp. Technol. Manag.* **2018**, *10*, e3018. [CrossRef]
55. Park, S.Y.; Cho, W.K.; Seol, W.S. A Mathematical Model of Liquid Rocket Engine Using Simulink. *Aerosp. Eng. Technol.* **2009**, *8*, 82–97.
56. Jung, T. Development and evaluation of startup simulation code for an open cycle liquid rocket engine. *J. Korean Soc. Propuls. Eng.* **2019**, *23*, 67–74. [CrossRef]
57. Jung, T. Transient Mathematical Modeling and Simulation for an Open Cycle Liquid Rocket Engine. In Proceedings of the Asia-Pacific International Symposium on Aerospace Technology, Jeju, Republic of Korea, 15–17 November 2021; pp. 1343–1360.
58. Yeon, K.B.; Insang, M. Study on Energy Balance at the Operating Points of Staged Combustion Cycle LRE. *Int. J. Aeronaut. Space Sci.* **2023**, 1–9.. [CrossRef]
59. Ha, C.; O, S.; Cha, J.; Ko, S. Basic modeling and analysis for the operation of Space Shuttle Main Engine. In Proceedings of the Korean Society for Aeronautical and Space Sciences Fall Conference, Jeju, Republic of Korea, 19–21 November 2014; pp. 1573–1576.

60. Lee, K.; Cha, J.; Ko, S.; Park, S.Y.; Jung, E. Mathematical modeling and simulation for steady state of a 75-ton liquid propellant rocket engine. *J. Aerosp. Syst. Eng.* **2017**, *11*, 6–12.
61. Cho, W.; Cha, J.; Ko, S.; Park, S.Y.; Jung, E. Development of MATLAB/Simulink Modular Simulation Environment for Open-cycle Liquid Propellant Rocket Engines. In Proceedings of the Korean Society for Aeronautical and Space Sciences Fall Conference, Jeju, Republic of Korea, 28 November–1 December 2018.
62. Cho, W.; Cha, J.; Ko, S. Development of MATLAB/Simulink Modular Simulation Toolbox for Space Shuttle Main Engine. *J. Korean Soc. Propuls. Eng.* **2019**, *23*, 50–60. [CrossRef]
63. Lee, S.; Jo, S.; Kim, H.; Kim, S.; Yi, S. A Numerical Study on the Simulation of Power-pack Start-up of a Staged Combustion Cycle Engine. *J. Korean Soc. Propuls. Eng.* **2019**, *23*, 58–66. [CrossRef]
64. Yu, S.; Jo, S.; Kim, H.; Kim, S.L. A 1-D Start-up Analysis for Liquid Rocket Engine Powerpacks. *J. Korean Soc. Combust.* **2019**, *24*, 39–45. [CrossRef]
65. Rachov, P.P.; Tacca, H.; Lentini, D. Electric feed systems for liquid-propellant rockets. *J. Propuls. Power* **2013**, *29*, 1171–1180. [CrossRef]
66. Lee, J.; Roh, T.S.; Huh, H.; Lee, H.J. Performance analysis and mass estimation of a small-sized liquid rocket engine with electric-pump cycle. *Int. J. Aeronaut. Space Sci.* **2021**, *22*, 94–107. [CrossRef]
67. Lee, J. Development of MS Program for Propellant Supply System of a Small-sized LRE with Electric-pump Cycle. Master's Thesis, Department of Aerospace Engineering, Inha University, Incheon, Republic of Korea, 2021.
68. Ramesh, D.; Aminpoor, M. Nonlinear, dynamic simulation of an open cycle liquid rocket engine. In Proceedings of the 43rd AIAA/ASME/SAE/ASEE Joint Propulsion Conference & Exhibit, Cincinnati, OH, USA, 8–11 July 2007; p. 5507.
69. Shafiey Dehaj, M.; Ebrahimi, R.; Karimi, H. Mathematical modeling and analysis of cutoff impulse in a liquid-propellant rocket engine. *Proc. Inst. Mech. Eng. Part G J. Aerosp. Eng.* **2015**, *229*, 2358–2374. [CrossRef]
70. Mahjub, A.; Mazlan, N.M.; Abdullah, M.; Azam, Q. Design optimization of solid rocket propulsion: A survey of recent advancements. *J. Spacecr. Rocket.* **2020**, *57*, 3–11. [CrossRef]
71. McDonald, A. Solid rockets-An affordable solution to future space propulsion needs. In Proceedings of the 20th Joint Propulsion Conference, Cincinnati, OH, USA, 11–13 June 1984; p. 1188.
72. Kim, Y.S.; Cha, J.H.; Ko, S.H.; Kim, D.S. Control of pressure and thrust for a variable thrust solid propulsion system using linearization. *J. Korean Soc. Propuls. Eng.* **2011**, *15*, 18–25.
73. Caubet, P.; Berdoyes, M. Innovative ArianeGroup Controllable Solid Propulsion Technologies. In Proceedings of the AIAA Propulsion and Energy 2019 Forum, Indianapolis, IN, USA, 19–22 August 2019; p. 3878.
74. Lombardo, G. Controllable Solid Propellant Rocket Motor Stability: Deep and Rapid Variable Thrust Operations. In Proceedings of the 44th AIAA/ASME/SAE/ASEE Joint Propulsion Conference & Exhibit, Hartford, CT, USA, 21–23 July 2008; p. 4608.
75. Park, I.S.; Lee, J.Y.; Choi, H.J.; Kim, J.H.; Yoon, H.G.; Lim, J.S. Pressure Control Law of Gas Generator Considering Combustion Volume Change. *J. Korean Soc. Propuls. Eng.* **2012**, *16*, 34–40.
76. Ki, T.; Ha, D.; Jin, J.; Lee, H.; Yoon, H. Analysis of Unsteady Combustion Performance in Solid Rocket Motor with Pintle. *J. Korean Soc. Propuls. Eng.* **2015**, *19*, 68–75. [CrossRef]
77. Hong, S. Gain Scheduling Controller Design and Performance Evaluation for Thrust Control of Variable Thrust Solid Rocket Motor. *J. Korean Soc. Propuls. Eng.* **2016**, *20*, 28–36. [CrossRef]
78. Cha, J.; de Oliveira, É.J. Performance Comparison of Control Strategies for a Variable-Thrust Solid-Propellant Rocket Motor. *Aerospace* **2022**, *9*, 325. [CrossRef]
79. Alan, A.; Yildiz, Y.; Poyraz, U. High-performance adaptive pressure control in the presence of time delays: Pressure control for use in variable-thrust rocket development. *IEEE Control Syst. Mag.* **2018**, *38*, 26–52. [CrossRef]
80. Bergmans, J.L.; Di Salvo, R. Solid rocket motor control: Theoretical motivation and experimental demonstration. In Proceedings of the 39th AIAA/ASME/SAE/ASEE Joint Propulsion Conference & Exhibit, Huntsville, AL, USA, 20–23 July 2003.
81. Lee, H.S.; Lee, D.Y.; Park, J.S.; Kim, J.K. A Study on Pressure Control for Variable Thrust Solid Propulsion System Using Cold Gas Test Equipment. *J. Korean Soc. Aeronaut. Space Sci.* **2009**, *37*, 76–81.
82. Ko, H.; Lee, J. Cold tests and the dynamic characteristics of the pintle type solid rocket motor. In Proceedings of the 49th AIAA/ASME/SAE/ASEE Joint PropulsionConference, San Jose, CA, USA, 14–17 July 2013; p. 4079.
83. Kwon, S.K.; Kim, Y.S.; Ko, S.H.; Suh, S.H. Pressure Control of a Variable Thrust Solid Propulsion System Using On-Off Controllers. In Proceedings of the Korean Society of Propulsion Engineers Conference, Busan, Republic of Korea, 2–24 November 2011; pp. 942–948.
84. Lee, J. A Study on the Static and Dynamic Characteristics of Pintle-Perturbed Conical Nozzle Flows. Ph.D. Thesis, Department of Mechanical Engineering, Yonsei University Seoul, Seoul, Republic of Korea, 2012.
85. Napior, J.; Garmy, V. Controllable solid propulsion for launch vehicle and spacecraft application. In Proceedings of the 57th International Astronautical Congress, Valenica, Spain, 2–6 October 2006; p. C4–2.
86. Lim, Y.; Lee, W.; Bang, H.; Lee, H. Thrust distribution for attitude control in a variable thrust propulsion system with four ACS nozzles. *Adv. Space Res.* **2017**, *59*, 1848–1860. [CrossRef]
87. Lee, H.; Bang, H. Efficient Thrust Management Algorithm for Variable Thrust Solid Propulsion System with Multi-Nozzles. *J. Spacecr. Rocket.* **2020**, *57*, 328–345. [CrossRef]

88. Ji, M.; Chang, H. Modeling and dynamic characteristics analysis on solid attitude control motor using pintle thrusters. *Aerosp. Sci. Technol.* **2020**, *106*, 106130.
89. Park, I.; Hong, S.; Ki, T.; Park, J. Pressure Guidance and Thrust Allocation Law of Solid DACS. *J. Korean Soc. Propuls. Eng.* **2015**, *19*, 9–16. [CrossRef]
90. Ki, T.; Hong, S.; Park, I.S. Dynamic Modeling and Characteristics Analysis of Solid Rocket Motor with Multi Axis Pintle Nozzles. *J. Korean Soc. Propuls. Eng.* **2015**, *19*, 20–28. [CrossRef]
91. Cha, J. A Study on Thrust Control System Design for Multi-Nozzle Solid Propulsion System. Master's Thesis, Department of Aerospace and Mechanical Engineering, Korea Aerospace University, Goyang, Republic of Korea, 2014.
92. Alan, A.; Yildiz, Y.; Poyraz, U. Adaptive pressure control experiment: Controller design and implementation. In Proceedings of the 2017 IEEE Conference on Control Technology and Applications (CCTA), Maui, HI, USA, 27–30 August 2017; pp. 80–85.
93. Yonggang, G.; Yang, L.; Zexin, C.; Xiaocong, L.; Chunbo, H.; Xiaojing, Y. Influence of lobe geometry on mixing and heat release characteristics of solid fuel rocket scramjet combustor. *Acta Astronaut.* **2019**, *164*, 212–229. [CrossRef]
94. Yang, L.; Yonggang, G.; Lei, S.; Zexin, C.; Xiaojing, Y. Preliminary experimental study on solid rocket fuel gas scramjet. *Acta Astronaut.* **2018**, *153*, 146–153. [CrossRef]
95. Chang, J.; Li, B.; Bao, W.; Niu, W.; Yu, D. Thrust control system design of ducted rockets. *Acta Astronaut.* **2011**, *69*, 86–95. [CrossRef]
96. Rezaei, H.; Soltani, M.R. An analytical and experimental study of a hybrid rocket motor. *Proc. Inst. Mech. Eng. Part G J. Aerosp. Eng.* **2014**, *228*, 2475–2486. [CrossRef]
97. Tahmasebi, E.A.; Karimi M, H. Conceptual design and performance simulation of a space hybrid motor. *Aircr. Eng. Aerosp. Technol. Int. J.* **2015**, *87*, 92–99. [CrossRef]
98. Chelaru, T.V.; Mingireanu, F. Hybrid rocket engine, theoretical model and experiment. *Acta Astronaut.* **2011**, *68*, 1891–1902. [CrossRef]
99. Gieras, M.; Gorgeri, A. Numerical modelling of the hybrid rocket engine performance. *Propuls. Power Res.* **2021**, *10*, 15–22. [CrossRef]
100. Cha, J.; Cho, W.; Lee, D.; Moon, H.; Ko, S. Mathematical modeling and simulation of a HDPE/Gox hybrid rocket motor. In Proceedings of the Korean Society for Aeronautical and Space Sciences Spring Conference, Goseong, Republic of Korea, 8–11 July 2020; pp. 310–311.
101. Tiensuu, K.; Hagel, E.; Bussmann, A.; Liljekvist, F.; Angeria, B.; Borg, L.; Coppa, E.; Gatti, F.; Williamson, A.; Athauda, D.; et al. RAVEN: A student rocket program at Luleå University of Technology, Sweden. In Proceedings of the 72nd International Astronautical Congress (IAC), Dubai, United Arab Emirates, 25–29 October 2021; International Astronautical Federation (IAF): Paris, France, 2021.
102. Kulu, E. Small launchers-2021 industry survey and market analysis. In Proceedings of the 72th International Astronautical Congress (IAC), Dubai, United Arab Emirates, 25–29 October 2021; International Astronautical Federation (IAF): Paris, France, 2021.
103. Genevieve, B.; Brooks, M.; Pitot de la Beaujardiere, J.; Roberts, L. Performance modeling of a paraffin wax/nitrous oxide hybrid rocket motor. In Proceedings of the 49th AIAA Aerospace Sciences Meeting including the New Horizons Forum and Aerospace Exposition, Orlando, FL, USA, 4–7 January 2011; p. 420.
104. Mungas, G.S.; Das, D.K.; Kulkarni, D. Design, construction and testing of a low-cost hybrid rocket motor. *Aircr. Eng. Aerosp. Technol.* **2003**, *75*, 262–271. [CrossRef]
105. Chae, H.; Chae, D.; Rhee, I.; Lee, C. Simulation of response characteristic of VTVL system with hybrid rocket engine. *J. Mech. Sci. Technol.* **2020**, *34*, 5239–5245. [CrossRef]
106. Bhadran, A.; Manathara, J.G.; Ramakrishna, P. Thrust control of lab-scale hybrid rocket motor with wax-aluminum fuel and air as oxidizer. *Aerospace* **2022**, *9*, 474. [CrossRef]
107. Whitmore, S.A.; Peterson, Z.W.; Eilers, S.D. Closed-loop precision throttling of a hybrid rocket motor. *J. Propuls. Power* **2014**, *30*, 325–336. [CrossRef]
108. Velthuysen, T.J. Closed-Loop Throttle Control of a Hybrid Rocket Motor. Master's Thesis, Department of Mechanical Engineering, University of KwaZulu-Natal, Durban, South Africa, 2018.
109. Peterson, Z.; Eilers, S.; Whitmore, S. Closed-loop thrust and pressure profile throttling of a nitrous-oxide HTPB hybrid rocket motor. In Proceedings of the 48th AIAA/ASME/SAE/ASEE Joint Propulsion Conference & Exhibit, Atlanta, GA, USA, 30 July–1 August 2012; p. 4200.
110. Peterson, Z.W. Closed-Loop Thrust and Pressure Profile Throttling of a Nitrous Oxide/Hydroxyl-Terminated Polybutadiene Hybrid Rocket Motor. Master's Thesis, Department of Aerospace Engineering, Utah State University, Logan, UT, USA, 2012.
111. Chae, D.; Chae, H.; Lee, C. Controlling plant dynamics change characteristics in thrust response of hybrid rocket engine. *J. Mech. Sci. Technol.* **2022**, *36*, 1537–1545. [CrossRef]
112. Schmierer, C.; Kobald, M.; Steelant, J.; Schlechtriem, S. Combined Trajectory Simulation and Optimization for Hybrid Rockets using ASTOS and ESPSS. In Proceedings of the 31st International Symposium on Space Technology and Science (ISTS), Matsuyama, Japan, 3–9 June 2017.

113. Rotondi, M.; Concio, P.; D'Alessandro, S.; Lucas, F.R.; Bianchi, D.; Nasuti, F.; Steelant, J. Development and Validation of Nozzle Erosion Models for Solid and Hybrid Rockets in the Espss Libraries. In Proceedings of the Conference: 8th Space Propulsion, Estoril, Portugal, 9–13 May 2022.
114. Lin, T.; Baker, D. Analysis and testing of propellant feed system priming process. *J. Propuls. Power* **1995**, *11*, 505–512. [CrossRef]
115. Hardi, J.S.; Oschwald, M.; Webster, S.C.; Gröning, S.; Beinke, S.K.; Armbruster, W.; Blanco, P.N.; Suslov, D.; Knapp, B. High frequency combustion instabilities in liquid propellant rocket engines: Research programme at DLR Lampoldshausen. In Proceedings of the Thermoacoustic Instabilities in Gas Turbines and Rocket Engines: Industry Meets Academia, Munich, Germany, 30 May–2 June 2016; pp. 1–11.
116. Schmidt, V.; Klimenko, D.; Haidn, O.; Oschwald, M.; Nicole, A.; Ordonneau, G.; Habbibalah, M. Experimental investigation and modelling of the ignition transient of a coaxial H2/O2-injector. In Proceedings of the 5th International Symposium on Liquid Rocket Propulsion, Chattanooga, TN, USA, 27–31 October 2003.
117. Bradley, M.; Bradley, M. Start with off-nominal propellant inlet pressures. In Proceedings of the 33rd Joint Propulsion Conference and Exhibit, Seattle, WA, USA, 6–9 July 1997; p. 2687.
118. Nam, C.H.; Park, S.Y. Gas Generator Cycle Liquid Rocket Engine Powerpack Startup Behavior Comparison by Valve Operation Order. In Proceedings of the Korean Society of Propulsion Engineers Fall Conference, Gyeongju, Republic of Korea, 5–6 December 2013; The Korean Society of Propulsion Engineers: Daejeon, Republic of Korea, 2013; pp. 566–560.
119. Park, S.Y.; Cho, W.K. Dispersion Analysis on the Startup and Shutdown Process of a Liquid Rocket Engine using Monte-Carlo Method. In Proceedings of the Korean Society of Propulsion Engineers Spring Conference, Busan, Republic of Korea, 28–29 May 2015; The Korean Society of Propulsion Engineers: Daejeon, Republic of Korea, 2015; pp. 787–791.
120. Cha, J.; Ko, S.; Park, S.Y.; Jeong, E. Fault detection and diagnosis algorithms for transient state of an open-cycle liquid rocket engine using nonlinear Kalman filter methods. *Acta Astronaut.* **2019**, *163*, 147–156. [CrossRef]
121. Wang, T.S. Transient two-dimensional analysis of side load in liquid rocket engine nozzles. In Proceedings of the 40th AIAA/ASME/SAE/ASEE Joint Propulsion Conference and Exhibit, Fort Lauderdale, FL, USA, 11–14 July 2004; p. 3680.
122. Wang, T.S. Transient three-dimensional startup side load analysis of a regeneratively cooled nozzle. *Shock Waves* **2009**, *19*, 251–264. [CrossRef]
123. Tomita, T.; Sakamoto, H.; Onodera, T.; Sasaki, M.; Takahashi, M.; Watanabe, Y.; Tamura, H. Experimental Evaluation of Side-load Characteristics on TP, CTP and TO nozzles. In Proceedings of the 40th AIAA/ASME/SAE/ASEE Joint Propulsion Conference and Exhibit, Fort Lauderdale, FL, USA, 11–14 July 2004; p. 3678.
124. Pérez-Roca, S.; Marzat, J.; Piet-Lahanier, H.; Langlois, N.; Farago, F.; Galeotta, M.; Le Gonidec, S. A survey of automatic control methods for liquid-propellant rocket engines. *Prog. Aerosp. Sci.* **2019**, *107*, 63–84. [CrossRef]
125. Nelles, O. *Nonlinear System Identification: From Classical Approaches to Neural Networks, Fuzzy Systems, and Gaussian Processes*; Springer Nature: Berlin/Heidelberg, Germany, 2020.
126. Santana, A., Jr.; Barbosa, F.; Niwa, M.; Goes, L. Modeling and robust analysis of a liquid rocket engine. In Proceedings of the 36th AIAA/ASME/SAE/ASEE Joint Propulsion Conference and Exhibit, Huntsville, AL, USA, 16–19 July 2000; p. 3160.
127. Santana, A.; Goes, L. Design and Dynamic Characteristics of a Liquid-Propellant Thrust Chamber. In Proceedings of the National Conference on Mechanical Engineering, Calcutta, India, 20–22 January 2000.
128. Jung, J.H. Modeling, and Classical and Advanced Control of a Solid Rocket Motor Thrust Vector Control System. Master's Thesis, Department of Electrical Engineering and Computer Science, Massachusetts Institute of Technology, Cambridge, MA, USA, 1993.
129. Karabeyoglu, M.A.; Altman, D. Dynamic modeling of hybrid rocket combustion. *J. Propuls. Power* **1999**, *15*, 562–571. [CrossRef]
130. Antoniou, A.; Akyuzlu, K. A physics based comprehensive mathematical model to predict motor performance in hybrid rocket propulsion systems. In Proceedings of the 41st AIAA/ASME/SAE/ASEE Joint Propulsion Conference & Exhibit, Tucson, AZ, USA, 10–13 July 2005; p. 3541.
131. Duyar, A.; Guo, T.H.; Merrill, W.C. Space shuttle main engine model identification. *IEEE Control Syst. Mag.* **1990**, *10*, 59–65. [CrossRef]
132. Nemeth, E.; Anderson, R.; Ols, J.; Olsasky, M. *Reusable Rocket Engine Intelligent Control System Framework Design, Phase 2*; Technical Report; The National Aeronautics and Space Administration: Los Angeles, CA, USA, 1991.
133. Dai, X.; Ray, A. Damage-Mitigating Control of a Reusable Rocket Engine: Part II—Formulation of an Optimal Policy. *J. Dyn. Syst. Meas. Control* **1996**, *118*, 409–415. [CrossRef]
134. Lv, X.; Zhang, M.; Ao, W.; Lin, Z.; Liu, P.; Cao, Y. AP/HTPB combustion response simulation with a new equivalent linear system method. *Combust. Flame* **2023**, *247*, 112486. [CrossRef]
135. Yang, E.f.; Zhang, Z.p.; Xu, Y.m. Nonlinear dynamic neural network model for rocket propulsion systems. *J. Propuls. Technol.-Beijing* **2001**, *22*, 50–53.
136. Le Gonidec, S.D. Method for Controlling the Pressure and a Mixture Ratio of a Rocket Engine, and Corresponding Device. U.S. Patent Application 15/750,311, 13 September 2018.
137. Lee, H.S.; Kwon, S.W.; Lee, J.S. Neural networks for the burn back performance of solid propellant grains. *Aerosp. Sci. Technol.* **2023**, *137*, 108283. [CrossRef]
138. Jung, M.Y.; Chang, J.H.; Oh, M.; Lee, C.H. Dynamic model and deep neural network-based surrogate model to predict dynamic behaviors and steady-state performance of solid propellant combustion. *Combust. Flame* **2023**, *250*, 112649. [CrossRef]

139. Zavoli, A.; Maria Zolla, P.; Federici, L.; Tindaro Migliorino, M.; Bianchi, D. Surrogate Neural Network for Rapid Flight Performance Evaluation of Hybrid Rocket Engines. *J. Spacecr. Rocket.* **2022**, *59*, 2003–2016. [CrossRef]
140. Zavoli, A.; Zolla, P.M.; Federici, L.; Migliorino, M.T.; Bianchi, D. Machine learning techniques for flight performance prediction of hybrid rocket engines. In Proceedings of the AIAA Propulsion and Energy 2021 Forum, Virtual, 9–11 August 2021; p. 3506.
141. Cha, J.; Ko, S. Modeling for transient state of open-cycle Liquid Propellant Rocket Engine using Method of Characteristics. In Proceedings of the Korean Society of Propulsion Engineers Spring Conference, The Korean Society of Propulsion Engineers, Jeju, Republic of Korea, 30 May–1 June 2018; pp. 391–395.
142. Cha, J.; Ko, S. Modeling of Space Shuttle Main Engine heat exchanger using Volume-Junction Method. In Proceedings of the Korean Society of Propulsion Engineers Spring Conference, The Korean Society of Propulsion Engineers, Jeju, Republic of Korea, 31 May–2 June 2017; pp. 213–217.
143. ESPSS (European Space Propulsion System Simulation). Available online: https://www.ecosimpro.com/products/espss/ (accessed on 28 March 2023).
144. Koppel, C.; Moral, J.; Steelant, J.; Perez Vara, R.; Omaly, P.; De Rosa, M. A platform satellite modelling with ecosimpro: Simulation results. In Proceedings of the 45th AIAA/ASME/SAE/ASEE Joint Propulsion Conference & Exhibit, Denver, CO, USA, 2–5 August 2009; p. 5418.
145. De Rosa, M.; Steelant, J.; Moral, J.; Elkouch, Y.; Pérez Vara, R. ESPSS: European Space Propulsion System Simulation. In Proceedings of the International Symposium on Propulsion for Space Transportation, Heraklion, Crete, 5–8 May 2008.
146. Hu, R.; Ferrari, R.M.; Chen, Z.; Cheng, Y.; Zhu, X.; Cui, X.; Wu, J. System analysis and controller design for the electric pump of a deep-throttling rocket engine. *Aerosp. Sci. Technol.* **2021**, *114*, 106729. [CrossRef]
147. Stepanoff, A.J. *Centrifugal and Axial Flow Pumps: Theory, Design, and Application*; Wiley: New York, NY, USA, 1957.
148. Yaman, H.; Çelik, V.; Değirmenci, E. Experimental investigation of the factors affecting the burning rate of solid rocket propellants. *Fuel* **2014**, *115*, 794–803. [CrossRef]
149. Gupta, G.; Jawale, L.; Mehilal, D.; Bhattacharya, B. Various methods for the determination of the burning rates of solid propellants: An overview. *Cent. Eur. J. Energetic Mater.* **2015**, *12*, 593–620.
150. Karabeyoglu, A.; Zilliac, G.; Cantwell, B.; De Zilwa, S.; Castellucci, P. Scale-up tests of high regression rate liquefying hybrid rocket fuels. In Proceedings of the 41st Aerospace Sciences Meeting and Exhibit, Reno, NV, USA, 6–9 January 2003; p. 1162.
151. Zilliac, G.; Karabeyoglu, M. Hybrid rocket fuel regression rate data and modeling. In Proceedings of the 42nd AIAA/ASME/SAE/ASEE Joint Propulsion Conference & Exhibit, Sacramento, CA, USA, 9–12 July 2006; p. 4504.
152. Greatrix, D.R. Regression rate estimation for standard-flow hybrid rocket engines. *Aerosp. Sci. Technol.* **2009**, *13*, 358–363. [CrossRef]
153. Kim, S.K.; Joh, M.; Choi, H.S.; Jeong, E. Calculation of Thermodynamic and Transport Properties of Kerosene Fuel Using NIST Surrogate Mixture Models. In Proceedings of the Korean Society of Propulsion Engineers Fall Conference, The Korean Society of Propulsion Engineers, Jeongseon, Republic of Korea, 21–23 December 2016; pp. 1146–1147.
154. Edwards, T.; Maurice, L.Q. Surrogate mixtures to represent complex aviation and rocket fuels. *J. Propuls. Power* **2001**, *17*, 461–466. [CrossRef]
155. Huber, M.L.; Lemmon, E.W.; Ott, L.S.; Bruno, T.J. Preliminary surrogate mixture models for the thermophysical properties of rocket propellants RP-1 and RP-2. *Energy Fuels* **2009**, *23*, 3083–3088. [CrossRef]
156. Chemical Equilibrium with Applications. Available online: https://www1.grc.nasa.gov/research-and-engineering/ceaweb/ (accessed on 28 August 2023).
157. McCarty, R.D. *Hydrogen Technology Survey: Thermophysical Properties*; Technical Report; National Bureau of Standards: Boulder, CO, USA, 1975.
158. Cha, J.; Ha, C.; Ko, S.; Koo, J. Application of fault factor method to fault detection and diagnosis for space shuttle main engine. *Acta Astronaut.* **2016**, *126*, 517–527. [CrossRef]
159. Cha, J.; Ko, S. Optimal Output Feedback Control Simulation for the Operation of Space Shuttle Main Engine. *J. Korean Soc. Propuls. Eng.* **2016**, *20*, 37–53. [CrossRef]
160. Gegeoglu, K.; Kahraman, M.; Ucler, C.; Karabeyoglu, A. Assessment of using electric pumps on hybrid rockets. In Proceedings of the AIAA Propulsion and Energy 2019 Forum, Indianapolis, IN, USA, 19–22 August 2019; p. 4124.
161. Liang, T.; Cai, G.; Wang, J.; Gu, X.; Zhuo, L.; Cao, L. A hydrogen peroxide electric pump for throttleable hybrid rocket motor. *Acta Astronaut.* **2022**, *192*, 409–417. [CrossRef]